Microelectronics Reliability 52 (2012) 762–782

Contents lists available at ScienceDirect

Microelectronics Reliability

journal homepage: www.elsevier.com/locate/microrel

Light emitting diodes reliability review

Moon-Hwan Chang [a], Diganta Das [a], P.V. Varde [a,c], Michael Pecht [a,b,*]

[a] CALCE Center for Advanced Life Cycle Engineering, University of Maryland, College Park, MD 20742, United States
[b] Center for Prognostics and System Health Management, City University of Hong Kong, Hong Kong, China
[c] Homi Bhabha National Institute, Reactor Group, Dhruva Complex, Bhabha Atomic Research Centre, Mumbai 400 085, India

ARTICLE INFO

Article history:
Received 21 February 2011
Received in revised form 9 July 2011
Accepted 16 July 2011
Available online 15 August 2011

ABSTRACT

The increasing demand for light emitting diodes (LEDs) has been driven by a number of application categories, including display backlighting, communications, medical services, signage, and general illumination. The construction of LEDs is somewhat similar to microelectronics, but there are functional requirements, materials, and interfaces in LEDs that make their failure modes and mechanisms unique. This paper presents a comprehensive review for industry and academic research on LED failure mechanisms and reliability to help LED developers and end-product manufacturers focus resources in an effective manner. The focus is on the reliability of LEDs at the die and package levels. The reliability information provided by the LED manufacturers is not at a mature enough stage to be useful to most consumers and end-product manufacturers. This paper provides the groundwork for an understanding of the reliability issues of LEDs across the supply chain. We provide an introduction to LEDs and present the key industries that use LEDs and LED applications. The construction details and fabrication steps of LEDs as they relate to failure mechanisms and reliability are discussed next. We then categorize LED failures into thirteen different groups related to semiconductor, interconnect, and package reliability issues. We then identify the relationships between failure causes and their associated mechanisms, issues in thermal standardization, and critical areas of investigation and development in LED technology and reliability.
© 2011 Elsevier Ltd. All rights reserved.

1. Introduction

Light emitting diodes (LEDs) are a solid-state lighting source increasingly being used in display backlighting, communications, medical services, signage, and general illumination [1–6]. LEDs offer design flexibility, from zero-dimensional lighting (dot-scale lighting) to three-dimensional lighting (color dimming using combinations of colors), with one-dimensional lighting (line-scale lighting) and two-dimensional lighting (local dimming, i.e., area-scale lighting) in between. LEDs have small exterior outline dimensions, often less than 10 mm × 10 mm. LEDs, when designed properly, offer high energy efficiency that results in lower power consumption (energy savings) with low voltage (generally less than 4 volts) and low current operation (usually less than 700 mA). LEDs can have longer life—up to 50,000 h—with better thermal management than conventional lighting sources (e.g., fluorescent lamps and incandescent lamps). LEDs provide high performance, such as ultra-high-speed response time (microsecond-level on–off switching), a wider range of controllable color temperatures (4500 K–12,000 K), a wider operating temperature range (−20 °C to 85 °C), and no low-temperature startup problems. In addition, LEDs have better mechanical impact resistance compared to traditional lighting. LEDs are also eco-friendly products with no mercury and low health impact due to low UV radiation. LEDs that have a single color are over ten times more efficient than incandescent lamps. White LEDs are more than twice as efficient as incandescent lamps [3].

LEDs range from a narrow spectral band emitting light of a single color, such as red, yellow, green, or blue, to a wider spectral band light of white with a different distribution of luminous intensity and spectrums and shades depending on color mixing and package design. A recent trend in LEDs to produce white light involves using blue LEDs with phosphors. White light is a mixture of all visible wavelengths, as shown in Fig. 1. Along with the prominent blue color (peak wavelength range 455–490 nm), there are other wavelengths, including green (515–570 nm), yellow (570–600 nm), and red (625–720 nm) that constitute white light. Every LED color is represented by unique x–y coordinates, as shown in Fig. 2. The CIE (Commission Internationale De L'eclairage (International Commission on Illumination)) chromaticity coordinates of x, y, and z are a ratio of the red, green, and blue stimulation of light compared to the total amount of the red, green, and blue stimulation. The sum of the RGB values ($x + y + z$) is equal to 1. The white area of the chromaticity diagram can be expanded, and boundaries are added to create each color range. The color temperatures and the Planckian locus (black body curve) show how they relate to the chromaticity coordinates [7].

* Corresponding author at: CALCE Center for Advanced Life Cycle Engineering, University of Maryland, College Park, MD 20742, United States. Tel.: +1 301 405 5323; fax: +1 301 314 9269.
E-mail address: pecht@calce.umd.edu (M. Pecht).

0026-2714/$ - see front matter © 2011 Elsevier Ltd. All rights reserved.
doi:10.1016/j.microrel.2011.07.063

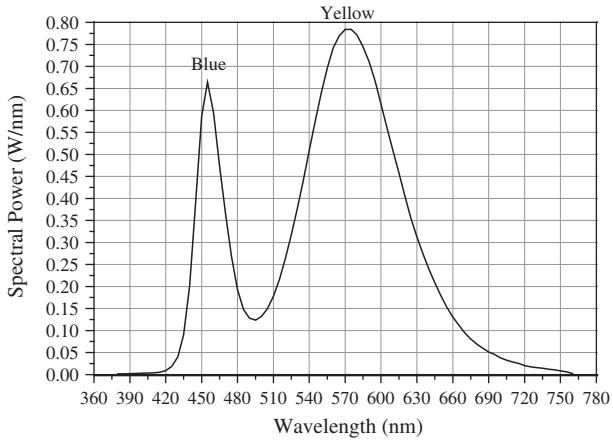

Fig. 1. Spectral power distribution for a white LED.

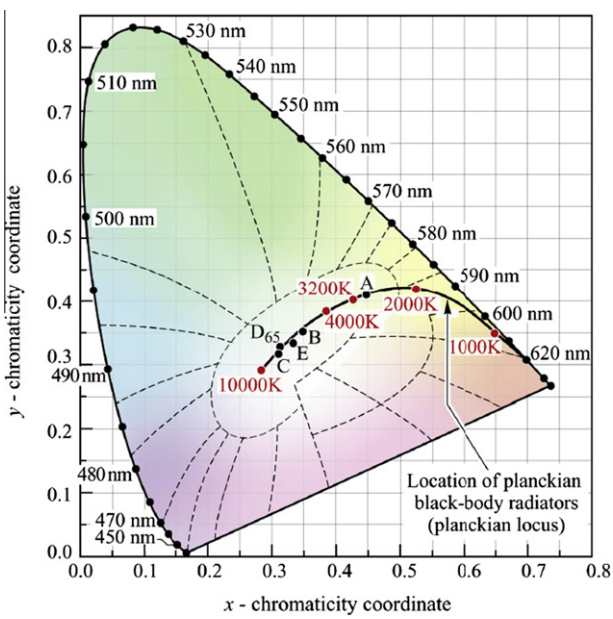

Fig. 2. CIE 1931 chromaticity diagram [8]. (© Cambridge University Press. Reprinted with permission.)

The color temperature of a white light is defined as the temperature of an ideal Planckian black-body radiator that radiates light of comparable hue to that white light source. The color temperature of light is equal to the surface temperature of an ideal black-body radiator in Kelvin heated by thermal radiation. When the black body radiator is heated to high temperatures, the heated black body emits colors starting at red and progressing through orange, yellow, white, and finally to bluish white. The Planckian locus starts out in the red, then moves through the orange and yellow, and finally enters the white region. The color temperature of a light source is regarded as the temperature of a Planckian black-body radiator that has the same chromaticity coordinates. As the temperature of the black body increases, the chromaticity location moves from the red wavelength range toward the center of the diagram in Fig. 2.

LED degradation not only results in reduced light output but also in color changes. LED modules are composed of many LEDs. This means that if some number of LEDs experience color changes, it will be noticed by users. Even if all of the LEDs degrade at the same rate, LED modules need to maintain their initial color, especially for indoor lighting and backlighting applications.

Table 1
Application areas of LEDs.

Application area	Application examples
LCD backlight	• Mobile phones • Cameras • Portable media players (PMPs) • Notebooks • Monitors • TVs
Displays	• Electric scoreboards • Outdoor billboards • Signage lighting
Transportation equipment lighting	• Vehicle/train lighting • Ship/airplane lighting
General lighting	• Indoor lighting • Outdoor lighting • Special lighting

LED application areas include LCD backlights, displays, transportation equipment lighting, and general lighting (see Table 1). LEDs are used as a light source for LCD backlights in products such as mobile phones, cameras, portable media players, notebooks, monitors, and TVs. Display applications include LED electronic scoreboards, outdoor billboards, and signage lighting, such as LED strips and lighting bars. Examples of transportation equipment lighting areas are passenger vehicle and train lighting (e.g., meter backlights, tail and brake lights) [9], and ship and airplane lighting (e.g., flight error lighting and searchlights). General lighting applications are divided into indoor lighting (e.g., LED lighting bulbs, desk lighting, and surface lighting) [10,11], outdoor lighting (e.g., decorative lighting, street/bridge lighting, and stadium lighting), and special lighting (e.g., elevator lighting and appliance lighting) [12,13]. The use of LEDs in general lighting has increased, beginning with street lighting in public areas and moving onto commercial/business lighting and consumer applications.

The history of LED development can be divided into three generations, each of which is characterized by distinct advancements in fabrication technology and equipment, development of new phosphor materials, and advancements in heat dissipation packaging technologies. Over time, LEDs have been becoming brighter, and color variance has been becoming more flexible. Light efficiency and light efficacy have also been improving. The first commercialized LED was produced in the late 1960s. This first generation of LEDs lasted from the 1960s until the 1980s. In this period, major application areas were machinery status indicators and alpha-numeric displays. The first commercially successful high-brightness LED (300 mcd[1]) was developed by Fairchild in the 1980s. In the second generation, from the 1990s to the present, high-brightness LEDs became popular. The main application areas for the second generation include motion displays, LED flashers, LED back light units (BLUs), mobile phones, automotive LED lighting, and architecture lighting. The third generation is now arriving in the market. These LEDs have been developed for substantial savings in energy consumption and reduction in environmental pollution. Future LED application areas are expected to include general lighting, lighting communication [14], medical/environmental fields, and critical applications in system controls. Some examples are portable LED projectors, large-size LED backlighting displays, LED general lighting, visible light communication, purifiers, and bio-medical sensors. Moore's Law predicts the doubling of the number of Si transistors in a chip every 18–24 months. Similarly, for LEDs, luminous output (luminous flux, measured in lm) appears to follow Haitz's Law,

[1] A monochromatic light source emitting an optical power of 1/683 watt at 555 nm into the solid angle of 1 steradian has a luminous intensity of 1 candela (cd).

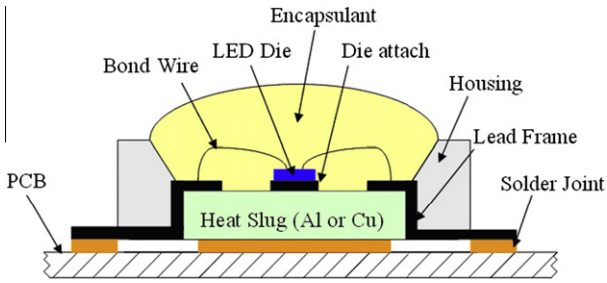

Fig. 3. LED package assembled with printed circuit board (PCB).

which states that LED flux per package has doubled every 18–24 months for more than 30 years [2]. This trend in the technological advancement of LEDs is based on industry-driven R&D efforts targeting high-efficiency, low-cost technology solutions that can successfully provide an energy-saving alternative to the recent applications of LEDs.

LED dies are composed of a p-junction, a quantum well (active layer) or multiple quantum wells, and an n-junction. LEDs emit light due to the injection electroluminescence effect in compound semiconductor structures. When a p–n junction is biased in the forward direction, electrons in the n-junction have sufficient energy to move across the boundary layer into the p-junction, and holes are injected from the p-junction across the active layer into the n-junction. The active region of an ideal LED emits one photon for every electron injected. Each charged quantum particle (electron) produces one light quantum particle (photon). Thus, an ideal active region of an LED has a quantum efficiency of unity. The internal quantum efficiency is defined as the number of photons emitted from an active region per second divided by the number of electrons injected into the LED per second. The light extraction efficiency is defined as the number of photons emitted into free space per second divided by the number of photons emitted from the active region per second [8,15]. Thus, the external quantum efficiency is the ratio between the number of photons emitted into free space per second and the number of electrons injected into the LED per second. Higher external quantum efficiency results in higher light output for the same amount of input.

The LED supply chain starts from an LED chip and progresses to an LED package, an LED module, and then to a system. LED production starts from a bare wafer made out of a material such as sapphire, GaN, SiC, Si, or GaAs. Many thin epilayers are grown on the bare wafer. Different colors of LEDs can be made by using different types of epiwafers. The types of epiwafer are InGaN/AlGaN for producing blue, green, and UV-range light; InAlGaP for producing red and yellow light; and AlGaAs for producing red or infrared-range light. The LED chip fabrication process involves attaching electric contact pads on an epiwafer and cutting the epiwafer into LED dies that are then packaged.

LEDs are classified into two types by color output: white LEDs and RGB LEDs. White LED packages can use red/green/blue/orange/yellow phosphors with blue LED chips to produce white light. The phosphors comprise activators mixed with impurities at a proper position on the host lattice. The activators determine the energy level related to the light emission process, thereby determining the color of the light emitted. The color is determined by an energy gap between the ground and excitation states of the activators in a crystal structure. RGB LED packages include red LED packages, green LED packages, blue LED packages, and LED packages with multi-dies in a single package producing white light using a combination of red, green, and blue LED dies.

A cross-sectional side view of white LEDs is shown in Fig. 3. An LED package mounted on a printed circuit board is composed of a housing, encapsulant, die, bond wires, die attach, lead frames, metal heat slug, and solder joints. The housing is a body for supporting and protecting the entire structure of an LED device. The housing is usually formed of materials such as polyphthalamide (PPA) or liquid crystal polymer (LCP). The encapsulant positioned over the housing is a resin material for the LED package in the shape of a dome. The typical material types for the resin are epoxy and silicon. The die is a compound semiconductor. The lead frames are used to connect the LED die to an electrical power source. The die attach is used to mechanically and thermally connect the chip to the heat slug. Typical types of die attaches are Ag paste and epoxy paste. Phosphors dispersed in the encapsulant emit white light when they are excited by absorbing a portion of the light from the LED dies.

LED types are placed in the following major categories depending on LED electrical power: low power LEDs are under 1 W of power (currents typically near 20 mA); medium power LEDs (high brightness LEDs) dissipate between 1 and 3 W of power (currents typically in the 30 mA/75 mA/150 mA range); and high power LEDs (ultra-high-brightness LEDs) have more than 3 W of power (currents typically in 350 mA/750 mA/1000 mA range). The LEDs vary because the LED current–voltage curves vary among materials.

The LED industry still faces challenges in attracting widespread consumption. One issue of concern is price, and another is lack of information regarding reliability. The number of LEDs required for an LCD BLU is an area where both of these issues converge. It may take from tens to sometimes thousands of LEDs to produce an LED BLU because the light emission of a single LED covers a limited area. If one single LED fails, the final product is sometimes treated as a failure. The failure of LEDs in an LCD display is critical, even when only a single LED package experiences changes in optical properties [16]. The failure of an LED or LEDs in an LCD display can cause a dark area or rainbow-colored area to appear on the LCD screen.

The LED die is a semiconductor, and the nature of manufacturing LED packages is similar to that of microelectronics. But there are unique functional requirements, materials, and interfaces in LEDs that result in some unique failure modes and mechanisms. The major causes of failures can be divided into die-related, interconnect-related, and package-related failure causes. Die-related failures include severe light output degradation and burned/broken metallization on the die. Interconnect failures of LED packages include electrical overstress-induced bond wire fracture and wire ball bond fatigue, electrical contact metallurgical interdiffusion, and electrostatic discharge, which leads to catastrophic failures of LEDs. Package-related failure mechanisms include carbonization of the encapsulant, encapsulant yellowing, delamination, lens cracking, phosphor thermal quenching, and solder joint fatigue that result in optical degradation, color change, electrical opens and shorts, and severe discoloration of the encapsulant. In this paper, the focus is on the failure sites, modes, and mechanisms at these three levels.

Cost is another barrier that confronts the LED industry in seeking to expand market share in general lighting. The current cost of LEDs ranges from $0.40 to $4 per package depending on the application. In the recent past, LEDs were often too expensive for most lighting applications. Even though the price of LEDs is decreasing quickly, it is still much higher than the price of conventional lighting sources. However, according to one study, the life cycle cost of an LED lighting system is less than for an incandescent lamp system [17]. The total cost of a lighting system includes the cost of electricity, cost of replacement, and the initial purchase price. Yet since the life cycle savings are not guaranteed at the time of lighting system selection, higher initial costs are still an obstacle to the acceptance of LED lighting. Reducing the manufacturing cost and selling price reduction while maintaining a high reliability level is key to increasing market share. According to a study by Samsung, the selling price of a white LED lighting system needs

to decrease by 50% in order to make LEDs more competitive with fluorescent lamp systems over the next 4–5 years [17].

2. LED reliability

End-product manufacturers that use LEDs expect the LED industry to guarantee the lifetime of LEDs in their usage conditions. Such lifetime information would allow LED designers to deliver the best combination of purchase price, lighting performance, and cost of ownership for the life of the end-products. One barrier to the acceptance of LEDs in traditional applications is the relatively sparse information available on their reliability. There are many areas in need of improvement and study regarding LEDs, including the internal quantum efficiency of the active region, light-extraction technology, current-flow design, the minimization of resistive losses, electrostatic discharge stability, increased luminous flux per LED package, and purchase cost [4]. Another barrier is the lack of globally accepted thermal standards, because all commercial properties of an LED-based system, such as light output, color, and lifetime, are functions of the junction temperature. More details can be found in Section 5.

It is rare for an LED to fail completely. LED lifetimes can vary from 3 months to as high as 50,000–70,000 h based on application and construction [18]. LED lifetime is measured by lumen maintenance, which is how the intensity of emitted light tends to diminish over time. The Alliance for Solid-State Illumination Systems and Technologies (ASSIST) defines LED lifetime based on the time to 50% light output degradation (L50: for the display industry approach) or 70% (L70: for the lighting industry approach) light output degradation at room temperature, as shown in Fig. 4 [19]. The accelerated temperature life test is used as a substitute for the room temperature operating life test to quickly predict LED lifetime. Prediction of LED lifetime varies with the method of interpreting the results of accelerated testing [20–22].

LED manufacturers usually perform tests in the product development cycle during the design and development phases. Typical qualification tests of LEDs are categorized into operating life tests and environmental tests by using industrial standards such as JEDEC or JEITA [23,24], which have been used by LED manufacturers such as Cree and Nichia. Operating life tests are performed by applying electrical power loads at various operating environment temperatures to LEDs to apply Joule heating to the internal parts of the LEDs. On the other hand, environmental tests are conducted with non-operating life tests. Tests vary among manufacturers. Generally, operating life tests for LEDs include the room temperature test, the high temperature test, the low temperature test, the wet/high temperature test, the temperature humidity cycle test, and the on/off test. Environmental tests of LEDs include the reflow soldering test, the thermal shock test, the temperature cycle test, the moisture resistance cyclic test, the high temperature storage test, the temperature humidity storage test, the low temperature storage test, the vibration test, and the electro-static discharge test. In some cases, combinations of these kinds of loading conditions are used. The acceptance criteria are pass or fail based on lumens, color, and electrical maintenance.

Environmental tests are utilized to determine the light output at initial test conditions and final test conditions. Data from other parameters are sometimes collected, such as chromaticity coordinate values (x and y) and reverse current when the lumen measurement is conducted at each data readout time. In many cases, the proper failure criteria of these other parameters are not defined to demonstrate how these collected data are correlated with the data from the light output degradation measurements.

LED system manufacturers are interested in estimating the expected duration of LEDs, since customers want the manufacturers to be able to guarantee a certain level of LED lifetime under usage conditions of the product, and manufacturers want to estimate the life cycle cost of LED systems. To achieve this, manufacturers usually perform accelerated life tests on LEDs at high temperatures while monitoring light output. Modeling of acceleration factors (AF) is generally used to predict the long-term life of LED packages at specific usage conditions [20,25]. A lifetime estimate is generally made using the Arrhenius model. Activation energy is sensitive to the test load condition, types of materials, and mechanical design of LED packages. The Arrhenius model estimates LED life with uncertainties such as exponential extrapolation of lifetime, assumed activation energy, possible failure mechanism shift between test and usage conditions, and discounting of all other failure causes besides temperature.

One method for predicting the lifetime of LEDs is the use of an accelerated test approach where the estimated lifetime in the accelerated life tests is multiplied by an acceleration factor. The process involves (1) measuring the light output of samples at each test readout time; (2) estimating LED life under the accelerated test conditions (using functional curve fitting of time-dependent degradation under the test conditions) or finding observed lifetime for L50 or L70, as shown in Fig. 4; (3) calculating an acceleration

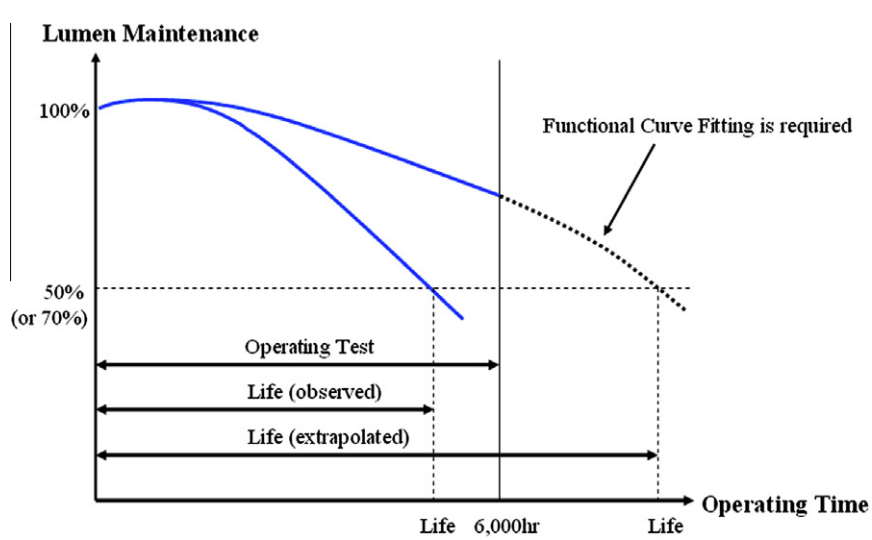

Fig. 4. Lifetime estimation based on LED accelerated life testing.

factor; and (4) predicting lifetime under the usage conditions by using the acceleration factor multiplied by the lifetime of the test condition, as shown in Eq. (1):

$$AF_{temp} = \exp\left[\frac{E_a}{k}\left(\frac{1}{T_u} - \frac{1}{T_a}\right)\right] \quad (1)$$

where E_a is the activation energy [eV], T_u is the junction temperature at usage conditions, T_a is the junction temperature at accelerated conditions, and k is the Boltzmann constant (8.6×10^{-5} eV/K).

The optical performance of an LED package is dependent on temperature. The junction temperatures in the active layers (quantum well structures) between the p–n junctions of the chip affect optical characteristics such as color and dominant wavelength. Direct measurement of the junction temperature is difficult, and the estimation of the junction temperature is derived from the LED case temperature or lead temperature. The luminous efficiency becomes low as the luminous flux emitted from an LED package decreases and the junction temperature increases. The junction temperature is dependent on the operating conditions (the forward current and the forward voltage) and operating environment. Light output measurement does not isolate the failure mechanisms of LEDs, because all failures affect light degradation. This current method of life testing (L50 or L70) may provide a basis for comparing the life expectancy of different LEDs, but it does not provide detailed information on the failure modes, failure mechanisms, and failure sites of LEDs. This method also does not help in remaining useful life estimation during operation.

Each LED lighting system manufacturer may use additional tests based on empirical development histories, applying previous product information to product development. Simple functional plotting in test conditions can be affected by the value of the activation energy of the Arrhenius model. This empirical curve plotting sometimes results in unclear data trending of LED lifetime even in the test conditions, since the functional curve fitting is very sensitive in terms of the number of samples and test duration [26–28]. There is a need to develop a more advanced life qualification tool that is able to predict the lifetime of a lighting system during the design, development, and early production phases using analytical tools, simulation, and prototype testing [29–36]. These techniques must be properly utilized in order to achieve improved reliability, increased power capability, and physical miniaturization [37–41].

LED lighting systems are needed to keep the light output and color of an LED constant throughout the lifetime of the LED by adjusting the amount of current when necessary. LED manufacturers usually specify a maximum current at each ambient temperature. Therefore, thermal feedback can be set to obtain the maximum current at a specific temperature. A major issue in high power LED applications involves the thermal cooling of systems. Currently, multiple temperature sensors, microprocessors, and/or amplifiers are utilized to reduce average LED current along a given maximum current vs. ambient temperature profile.

LED circuit designs on printed circuit boards also need to be controlled to maintain the electrical and optical stability of LEDs [31,42–46]. Systems for driving LEDs are generally composed of AC–DC power supplies, a DC–DC converter, intelligent controllers, an LED driver, and an LED board to maintain the light output and color of LEDs [47,48]. For lighting system design, one must take into account the following: the ability to save space on and reduce the PCBs by integrating components; the level of flexibility needed to add features and adapt to last minute changes; and the compatibility for interfacing different types of sensors with current designs. In the case of outdoor lighting applications, an intelligent controller may not be required because color change is not as critical of a problem as it would be in an LED display backlighting system. An intelligent controller enables binning/temperature compensation, color temperature control, and color control of the lighting system via the color sensor and temperature sensor. The intelligent controller includes programmable digital blocks and analog blocks. These blocks are interfaced with external sensors for collecting censored/amplified data and filtering the data out to perform feedback input. LED drivers generate constant current to light up each LED string. LED driver circuits are composed of current sense amplifiers (feedback elements), hysteretic controllers (control function), internal n-channel MOSFETs (switches), gate drivers for driving external n-channel MOSFETS, n-bit hardware PWMs/PrlSMs/DMMs (modulation), hardware comparators (protection and monitoring), hardware DACs (protection and monitoring), a switching regulator, and a dedicated port of IOs to connect to power peripherals and GPIO (general purpose input/output) functionality [47]. The intelligent controller and LED driver can be embedded into one circuit board for cost savings, smaller PCB size, and intelligent lighting design for tunable white light and mixed-color light operations.

The ways to drive the current to light up LEDs are divided into pulsed width modulation (PWM) dimming and analog dimming (amplitude dimming) [49]. Analog dimming involves changing the constant current through the LED by adjusting the sense voltage. Analog dimming does not generate additional switching noise in the LED lighting system and has higher efficacy as current levels decrease. The dominant wavelength varies with LED current due to band filling and the quantum-confined Stark effect (QCSE), so some color shift is to be expected when using analog dimming. On the other hand, PWM dimming involves a desired LED current and can turn the LED on and off at speeds faster than the human eye can detect. The color of LEDs can be controlled by using PWM dimming if the junction temperature is controlled, since the dominant wavelength changes due to the junction temperature. The input supply needs to be filtered properly to accommodate high input current transients. The efficiency of PWM dimming is lower than that of analog dimming [49]. PWM dimming technology is categorized into enable dimming, series dimming, and shunt dimming. Enable dimming produces PWM current by turning on and off the current. Enable dimming is easy to implement, but typically shows slow current transitions. Series dimming uses the series field effect transistor (FET) to generate PWM current with current transition. Output voltage can overshoot when using series dimming. Shunt dimming utilizes shunt FET to generate the PWM signal with super-fast current transitions. The drawback of shunt dimming is that power is dissipated in the shunt FET. If it is necessary to drive different types of LEDs having different forward voltages, multi-boost or buck current mode control is used due to the benefit of independent multiple power stages. PWM dimming control is good for driving uniform LEDs with the same color and forward voltages [48]. Although, the reliability and performance of these control circuits are critical to the success of LED lighting systems, this paper covers only LED packages.

3. Failure modes and mechanisms in LEDs

In this paper, the failure mechanisms of LEDs are divided into three categories: the semiconductors, interconnects, and the package. Semiconductor–related failure mechanisms include defect and dislocation generation and movement, die cracking, dopant diffusion, and electromigration. Interconnect-related failure mechanisms are electrical overstress–induced bond wire fracture and wire ball bond fatigue, electrical contact metallurgical interdiffusion, and electrostatic discharge. Package-related failure mechanisms include carbonization of the encapsulant, delamination, encapsulant yellowing, lens cracking, phosphor thermal quenching, and solder joint fatigue. This section discusses the various failure mechanisms of LEDs.

3.1. Semiconductor-related failure mechanisms: defect and dislocation generation and movement

The lifetime and performance of LEDs are limited by crystal defect formations in the epitaxial layer structure of the die [50–53]. Crystal defects are mainly generated in contacts and in the active region [54]. Crystal defects result in a reduction in the lifetime [55] of non-equilibrium electron hole pairs and an increase in multi-phonon emissions under high drive currents [56–60]. Multi-phonon emissions result in the strong vibration of defect atoms and reduce the energy barrier for defect motions, such as migration, creation, or clustering [60].

The failure modes are light output degradation due to nonradiative recombination at defects and shifted electrical parameters due to increased reverse leakage currents. Electrical failure modes known for this failure mechanism include an increase in the reverse leakage current along with optical power degradation, an increase in the generation-recombination current at low forward bias, an increase in the diode ideality factor, and an increase in parasitic series resistance. For a perfect diode, the ideality factor is unity (1.0). For real diodes, the ideality factor usually assumes values between 1.1 and 1.5. However, values as high as 7.0 have been found for GaN/InGaN diodes [61]. Parasitic series resistance is related to a semiconductor's ohmic contact degradation on top of the p-layer. Parasitic resistance induces high-current crowding effects that increase the current during DC aging tests at different current levels [56,57]. In the case of GaAlAs/GaAs LEDs, even moderate dislocation densities ($\sim 10^4$ cm^{-2}) can affect the operating life of LEDs, and the degradation rate related to the dislocation motion is high [62]. On the other hand, the degradation rates of InGaAsP/InP and InGaN LEDs are slow compared to GaAlAs/GaAs LEDs since the defects have no deep trap levels in the band gap and they do not act as nonradiative recombination centers as do GaAlAs/GaAs LEDs [62,63].

Defects introduced during crystal growth are divided into interface defects and bulk defects [64]. Interface defects include stacking faults, V-shaped dislocations, dislocation clusters, microtwins, inclusions, and misfit dislocations. Bulk defects include defects propagating from the substrate and those generated by local segregation of dopant atoms or native point defects. Structural imperfections due to thermal instability also contribute to defect generation during crystal growth. Degradation modes of defect generation in LED dies are divided into rapid degradation (random or sudden unpredicted degradation) and gradual degradation (wearout degradation). Recombination-enhanced dislocation climb and glide are responsible for rapid degradation [65]. One example of gradual degradation is the exits due to the recombination-enhanced point defect reaction in GaAlAs/GaAs-based optical devices. Internal stress due to lattice mismatch also causes gradual degradation [60,66].

Gradual degradation proceeds as follows. First, nonradiative recombination occurs in a defect, which causes a point-defect reaction and new point-defect generation. The new defects can also act as non-radiative recombination centers. The generated point defects migrate and condense at nucleation centers. Defect clusters and/or microloops are formed as byproducts [64]. Chuang et al. found that four actions are continuously repeated when an electron is captured with a hole at a defect site. This causes strong defect vibrations and results in defect generation [60]. The four actions are electron–hole non-radiative recombination at defect sites, the release of band gap energy via multi-phonon emissions, strong vibration at defect sites, and defect diffusion and generation.

Ferenczi reported that gradual performance degradation is mainly concerned with the formation of new non-radiation recombination sites, leading to a decrease in the radiative quantum efficiency [67]. If the nonradiative recombination centers form at interfaces, the increased interface density of states leads to erratic switching drawbacks and finally dislocation movement and increased dislocation concentration. This results in mechanical stress fields when dislocation concentration increases greatly.

The dislocation velocity (V_d) of semiconductors is known to depend on applied shear stress (τ) [62,63]:

$$V_d = \tau\mu \tag{2}$$

$$\mu = V_0/\tau_0 \exp(-E_d/kT) \tag{3}$$

where μ is the dislocation mobility, E_d is the activation energy of dislocation motion, T is the temperature, and V_0 and τ_0 are pre-exponential factors. It has been reported that GaN-based LEDs are more reliable than GaAs-based LEDs in high density dislocations [63]. The applied shear stress (τ) is affected by internal misfit strain, thermal strain, and external mechanical strain. Three types of dislocations of GaN-based LEDs are observable by cross-sectional transmission electron microscopy (XTEM), as schematically illustrated in Fig. 5 [63]. Type 1 dislocations are wing-shaped 60° or screw dislocations on the basal (0 0 0 1) plane. Type 2 dislocations are straight threading edge dislocations existing on $\{1\,\overline{1}\,0\,0\}$ planes. Type 3 dislocations are the dislocations that remain on the buffer layer. Failure analyses for defect and dislocation generation and movement were followed by electrical current voltage (I–V) characteristics and capacitance–voltage (C–V) measurements, deep-level transient spectroscopy (DLTS) analyses, and optical device emission measurements made by using the complementary techniques of electroluminescence (EL) and cathodoluminescence (CL) to detect different excitation mechanisms and power regimes as well as efficiency decrease during stress [68].

Threading dislocations form at the interface of the substrate and epitaxial layer. These propagate toward the surface of the epitaxial layer and are often called micropipes because of their open core nature. Threading dislocations form in highest density on sapphire-based GaN LEDs [69,70].

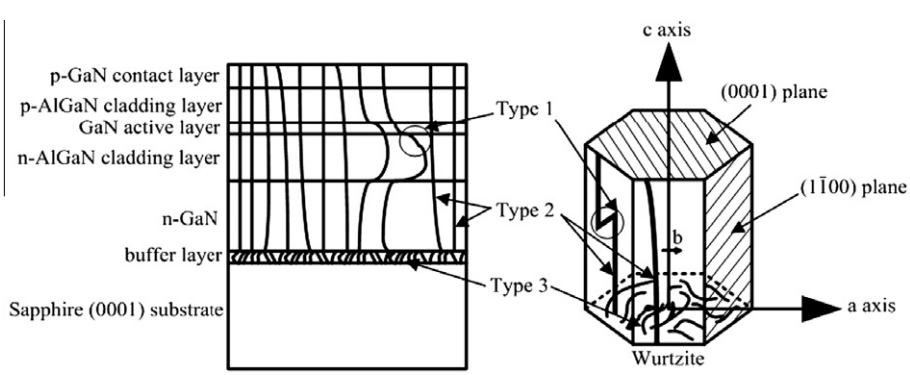

Fig. 5. Schematic diagram of types of dislocations in GaN-based LEDs [63]. (© American Institute of Physics. Reprinted with permission.)

Pan et al. reported that current-induced thermal effects play a role in the luminescence efficiency of UV LEDs under DC and pulsed injection. The thermal effects affect the redshifted luminescence wavelength of DC-driven devices. Pan et al. found that the failure of UV LEDs was due to carrier overflow and nonradiative recombination through threading dislocation [71]. Pavesi et al. reported that failures of structural properties (defects, unintentionally incorporated impurities, and doping) are due to electro-thermal stress [72]. Pavesi et al. also discussed the temperature and current dependencies of the electrical activity of localized defects and their effects on the electroluminescence efficiency of InGaN-based blue LEDs [73].

Cao et al. investigated electrical and optical degradation of GaN/InGaN single-quantum-well LEDs under high injection current and reverse-bias stress [74]. Gradual changes in light output power-current–voltage characteristics showed the slow formation of point defects, which enhance nonradiative recombination and low-bias carrier tunneling. Cao et al. proposed two different models for defect generation. Defect generation under high forward-current stress results from a thermally assisted and recombination-enhanced process in the InGaN layer. The defect generation under high reverse voltage changes the material, resulting in avalanche breakdown at the boundaries between the space-charge region and pre-existing microstructural defects.

Future research on defect and dislocation generation and motion will require improved structural and material design of LED dies and improved internal thermal management handling of thermal resistance from junction to the package to reduce the formation of crystal defects and dislocation movements caused by high-current-induced thermal effects and high ambient temperature.

3.2. Semiconductor-related failure mechanisms: die cracking

Extreme thermal shocks can break the dies of LEDs, such as GaN-based and GaAs-based LED dies. Due to differences in material properties (such as the coefficient of thermal expansion), LED packages can be subjected to mechanical stress when a high drive current is applied (which causes Joule heating at a fast rate) or when high ambient temperature conditions are suddenly applied [15]. The high electrical stress and extreme thermal shock are the causes of die cracking [15,52,56]. It is necessary to control die cracking by fine-tuning thermal expansion coefficients between the substrate and epitaxial layers, as shown in Fig. 6. The growth of the optimal medium layer between the substrate and the epitaxial layer is a key technology to prevent die cracking [75].

In some cases, the failure mode from die cracking can be electrical degradation and not, as intuitively expected, overstress failure. Barton et al. [75] found that the light output degradation was due, not to a change in contact resistance or the optical transmission of the plastic encapsulation, but to die cracking. Electron beam–induced voltage (EBIV) analysis showed that the light output degradation was due to a crack propagated through the p-contact and the active layer in the LED die, thus isolating part of the junction area from the p-contact. The sawing and grinding quality of the die has a significant impact on the occurrence of die crack [76,77]. Initial defects, such as tiny notches or micro-cracks, caused by the sawing and/or grinding process may act as a starting point for die cracking. Chen et al. reported that the strength of LED dies cut from wafers has to be determined for the needs of the design in order to assure the good reliability of the packages in manufacturing and service [78].

3.3. Semiconductor-related failure mechanisms: dopant diffusion

To produce a high brightness GaN-based LED, efficient current injection into the LED through the p-GaN layer is usually required. The p-GaN layer needs the improvement of the hole concentration of the p-GaN layer as well as the conductivity in order to decrease the resistivity of the p-type Ohmic contact [79–86]. For the p-type GaN, Mg is used as the acceptor [87] in order to inject the current into LEDs efficiently. Si is generally used in the growth process of GaN as an n-type dopant. When Mg diffuses into the quantum well during the growth of the p-GaN layer it causes the lowering of the internal quantum efficiency of the multiple quantum well (MQW) as the Mg acts as the nonradiative recombination center [88]. The effect of the distribution of Mg dopant into the quantum well is called dopant diffusion. The Mg doping profile close to the active region was found to be influenced by segregation as well as by diffusion during growth.

Kohler et al. investigated the influence of the Mg doping profile on the electroluminescence (EL) efficiency of (AlGaIn)N quantum well LEDs grown by low-pressure metal–organic vapor phase epitaxy [88]. They found that high Mg concentrations close to the active region that started at low growth temperatures increased EL efficiency because of improved hole injection. Conversely, high Mg concentrations close to the GaInN QWs increase nonradiative recombination rates. Kwon et al. [89] further reported that the performance of InGaN–GaN MQW ultraviolet LEDs was enhanced by gradient doping of Mg in the p-GaN layer, because the gradient doping is able to decrease the Mg diffusion into an MQW active layer. The performance enhancement is also due to the reduction in undesirable carrier transition from the conduction band of the MQW to the acceptor level in the p-GaN:Mg layer. Altieri-Weimar et al. stated that the amount of magnesium (in the active layer for p-doping) and tellurium doping (in the n-doped layers for n-doping), as well as of the amount of oxygen incorporation, influence red–orange AlGaInP LED degradation [90]. The authors also reported that high stress aging temperatures over 85 °C can accelerate Te-doped AlGaInP LED degradation.

During life tests, failure modes caused by dopant diffusion acting as nonradiative recombination center include an increase in series resistance and/or forward voltage, which is accompanied by increased current crowding effects; an increase in the tunneling

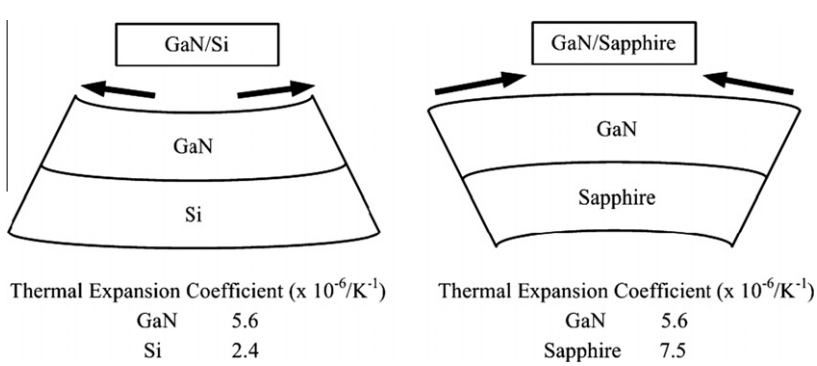

Fig. 6. Thermal expansion coefficients of GaN/Si and GaN/sapphire.

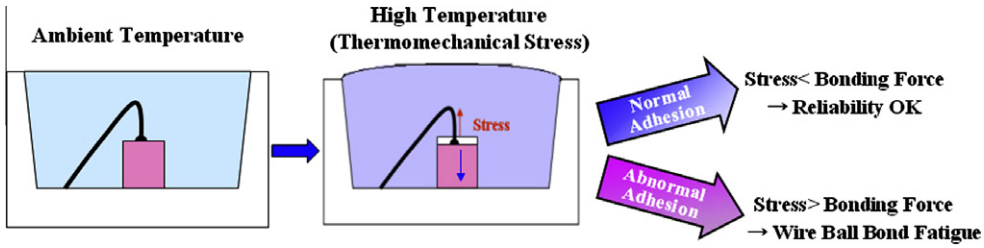

Fig. 7. Wire ball bond fatigue.

effect of forward diode current and reverse current; and degradation of optical intensity. The general failure mode is decreased light output. Instabilities in the p-type GaN layers as well as the growth of nonradiative recombination centers degrade the optical power emitted. The primary causes of light degradation are current density, temperature, and current distribution, which causes an increase in series resistance [72,91–93].

3.4. Semiconductor-related failure mechanisms: electromigration

Electromigration is electrically induced movement of the metal atoms in the electrical contact to the surface of the LED die (such as GaN-based and GaAs-based LED dies) due to momentum exchange with electrons. Inadequately designed LEDs may develop areas of lower and higher thermal resistance (and temperature) within the substrate due to defects, electromigration, or incomplete soldering. This leads to current crowding, causing thermal runaway, which results in severely increasing temperature in the package [69] and reduction of the life of LEDs.

Electromigration causes contact migration between the electrical contact and the surface of the LED die, which leads to a short circuit. The driving force is either high drive current or excessive current density. In sources with electrodes, degradation of the LED is due to the metal diffusing towards the inner region [59,94]. During operation the metal diffuses from the p-contact across the junction, creating spikes along the direction of current flow. Electromigration of contact metals occurs along crystalline defects or defect tubes.

Kim et al. [95] showed the growth of a dot spot on the electrode surface due to electromigration, which consequently resulted in short circuit failure under various stress conditions. Their results showed the increase of forward and reverse leakage current after electrical stress, which was evidence of contact electromigration. Haque et al. [96] reported that materials selection having chemical compatibility should be considered when seeking to mitigate electromigration failures. Barton et al. [97] found that electromigration of contact metals in GaN-based blue LEDs was along crystalline defects or defect tubes. A degradation study by Barton et al. [98] on an InGaN green LED under high electrical stress found that the degradation was fast (about 1 s) when the pulsed current amplitude was increased above 6 A and 100 ns pulse width at a repetition rate of 1 kHz with a visible discharge between the p- and n-type electrodes. This led to the creation of shorts in the surface plane of the diode, resulting in damage to metal contacts.

Proper thermal management and innovative package designs are required to solve electromigration. Thermal conductivities of interface materials, which constitute a large portion of the thermal resistance, should be improved to prevent electromigration because the contact resistances of the interface materials can affect the overall thermal resistance. In addition, low thermal conductivity control at high ambient temperature must be taken into account in the design process.

3.5. Interconnect-related failure mechanisms: electrical overstress-induced bond wire fracture and wire ball bond fatigue

Wire bonding is the most common method for connecting the pads on a chip to those on the LED packages. When LED packages are exposed to high forward currents or high peak transient currents, the bond wire can behave as a fuse [15]. Electrical overstress usually causes bond wire fracture, where the wire is instantly broken above the wire ball. This can cause catastrophic failure [99]. The severity of electrical overstress-induced bond wire fracture is related to the amplitude and duration of the electrical transients and the diameter of the bond (usually gold) wire [15]. Very long pulse duration of electrical transients and high DC forward current also result in thermomechanical stress–related failures.

Wire ball bond fatigue by thermomechanical stress is a type of wear-out failure mechanism. Repetitive, high-magnitude thermal cycles can lead to rapid failure. The thermal expansion of the encapsulant pulls the wire bond from the surface of the die [52,69,101]. Wire ball bond fatigue takes place when thermomechanical stress drives the repetition of thermal expansion and contraction of the expanding materials, as depicted in Fig. 7. A wire ball open occurs when the thermomechanical stress is higher than the wire ball bonding force. At elevated temperatures, the level of the thermal expansion coefficient and the Young's modulus of the encapsulant, as well as the hardness of the die, affects wire ball bond fatigue. The mismatch of coefficients of thermal expansion (CTEs) causes the wire bond and chip to generate a significant thermomechanical stress in the bonding zone. This results in fatigue crack propagation during thermal cycling. The reliability of such a joint varies with bond wire length and loop height [102]. Long-term exposure to a high humidity environment can also result in wire ball bond fatigue. When the quantity of absorbed water molecules within the epoxy encapsulant is of sufficient density to chemically attack the top electric contact on the LED die, the wire bond on the chip breaks the connection [100].

The bonding process should be optimized by controlling wire type, pad metallization, and device configurations. Accurate bonding tests have to be performed by varying bonding parameters such as clamping force, power, and time matching bond pull strength to extract optimum bonding conditions. The chip damage under the bonding strength conditions should also be minimized.

3.6. Interconnect-related failure mechanisms: electrical contact metallurgical interdiffusion

Electrical contact metallurgical interdiffusion is caused by thermally activated metal–metal and metal–semiconductor interdiffusion [103,104]. A schematic diagram of the structure of an AlGaN/InGaN/AlGaN LED is illustrated in Fig. 8. Electrical contact metallurgical interdiffusion differs from electromigration in the sense that electrical contact degrades due to out-diffusion and in-diffusion of the electrical contact. On the other hand, electromigration

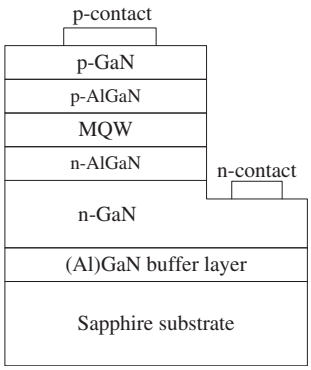

Fig. 8. Structure of a GaN-based LED die.

is due to crystalline defects or defect tubes forming in the metal and places where metal atoms accumulate. The continuous metallurgical interdiffusion causes electrical contact degradation, which results in the alloying and intermixing of the contact metals.

For example, in a AuGe/Ni contact, nonstochiometric regions are formed when Ga diffuses outward through the AuGe into the Au layer, while Au diffuses inward, forming high resistive alloying, which causes the contact resistance to increase [105]. The failure modes of the electrical contact metallurgical interdiffusion of LED packages are light output degradation, an increase in parasitic series resistance, and short circuits of LEDs. The driving forces of failures are high drive current and high temperature increase.

Meneghesso et al. [56] stated that the long-term reliability of GaN/InGaN under DC-aged testing showed semi-transparent Ohmic contact degradation on top of the p-layer, which resulted in an increase in the parasitic series resistance and light output degradation. The increase in the parasitic series resistance induces increasingly harsh current crowding effects as the current increases during the tests. The values of the parasitic series were evaluated from the current–voltage curves. At high voltages under extreme DC-aging tests, an increase in the parasitic series resistance was found [58]. An electrothermal degradation study on InGaN LEDs by Pavesi et al. [72] also showed that LEDs electrically stressed at 100 mA without a heat sink experienced a decrease in light output up to 70% after 500 h, with an increase in the series resistance and forward voltage as well as with the current crowding effects observed by emission microscopy. Meneghini et al. [106] analyzed the degradation of p-GaN contacts degraded under high-temperature storage at 250 °C. High temperature storage induced a voltage increase and the nonlinearity of the electrical characteristics around zero voltage in the *I–V* curves.

3.7. Interconnect-related failure mechanisms: electrostatic discharge

Electrostatic discharge (ESD) is a type of failure mechanism resulting in rapid open circuit failure in LEDs (such as GaN-based diodes) with sapphire substrates, which are commonly used in blue, green, and white LEDs. The forward biased pulse (1 ns to 1 μs) usually passes through the LED without damage, but a reverse biased pulse causes electrostatic discharge. Breakdown voltage and reverse saturation current are affected by contact material, thickness, defects in the substrate, and contamination [52,100].

One possible solution is a correctly rated Zener diode reverse biased in parallel with the LED [52,107]. This device allows voltage spikes to pass through the circuit in both directions without damage to the LED. Another solution incorporating an internal GaN Schottky diode into the LED chips improved ESD characteristics of nitride-based LEDs [108,109]. Inverse-parallel shunt GaN ESD diodes also improve the ESD reliability of GaN-based LEDs [110]. SiC substrates, GaN substrates, and Si substrates with high thermal resistance can also improve ESD robustness.

A sapphire substrate is electrically insulated. The p- and n-contacts are generally positioned on the same side. GaN/InGaN devices are easily damaged by electrostatic discharge and power dissipation because the sapphire substrate has low thermal resistance because of the insulation effect [111,113,114]. Su et al. showed that an LED with a 1040 °C-grown p-cap layer can endure ESD pulses up to 3.5 kV [111]. Their experiments demonstrated that ESD performances of LEDs are sensitive to V-shaped defects and bonding pad design. The forming of V-shaped pits on the p-GaN top layer is also related to the surface termination of threading dislocations [112]. These V-shaped pits cause a leakage path, which leads to worse electrostatic discharge (ESD) characteristics. The results of Tsai et al. [112] demonstrated that GaN-based LEDs with a high-temperature-grown p-GaN layer can withstand a negative electrostatic discharge voltage of up to 7 kV. Zhang et al. [113] reported that the fabricated flip-chip light-emitting diodes (FCLEDs) tolerated 10 kV ESD shock by embedding Zener diodes connected in parallel with the LED die. SiC substrate improved ESD robustness by reducing lattice mismatch in reverse bias conditions [114]. A modulation-doped $Al_{0.12}Ga_{0.88}N$/GaN superlattice improved ESD reliability in nitride-based LEDs by spreading pulse current when LEDs suffered from ESD [115].

3.8. Package-related failure mechanisms: carbonization of the encapsulant

Carbonization of the plastic encapsulation material on the diode surface under electrical overstress resulting in Joule heating or high ambient temperatures leads to the formation of a conductive path across the LED and subsequently to the destruction of the diode itself. Carbonization of the encapsulant decreases the encapsulant's insulation resistance, significantly inhibiting its ability to provide electrical insulation between adjacent bondwires and leads [116]. The loss in insulation resistance of the plastic combined with latch-up of the device at temperatures above threshold temperature (such as 200 °C of high ambient temperature for plastic-encapsulated microcircuits) can initiate a thermal runaway process leading to carbonization of the encapsulant. In this process, the fusing of the bondwires at high current causes the current to be shunted through the plastic, leading to Joule heating of the plastic. This Joule heating further decreases the insulation resistance and can eventually result in carbonization of the encapsulant [117]. The failure mode of carbonization of the encapsulant is light output degradation. The failure site is shown in Fig. 9.

Failure analysis results for the degradation of single-quantum-well InGaN LEDs under high electrical stress indicate that the degradation process begins with carbonization of the plastic encapsulation material on the diode surface [103]. Meneghesso et al. reported that plastic carbonization was present along the bond wire, suggesting power or temperature-related encapsulant degradation, which could contribute to optical power degradation [118]. In the degradation process, the encapsulant packaging material burns and leaves a conductive carbon film on the die [119–121]. Several black spots detected on the p-contact layer of the LED die were burned plastic areas generated when the junction below them went into a non-constant breakdown under high pulsed electrical stress. Continued stress started to create the conductive layer, forming a short circuit across the LED die. Further application of electrical stress caused catastrophic package failure.

Fine-tuning of absolute maximum ratings of electrical current and ambient temperature for usage conditions as well as thermal management are required to avoid unexpected high loads resulting in carbonization of the encapsulant. As a safety margin, derating guidelines can also be provided to the users.

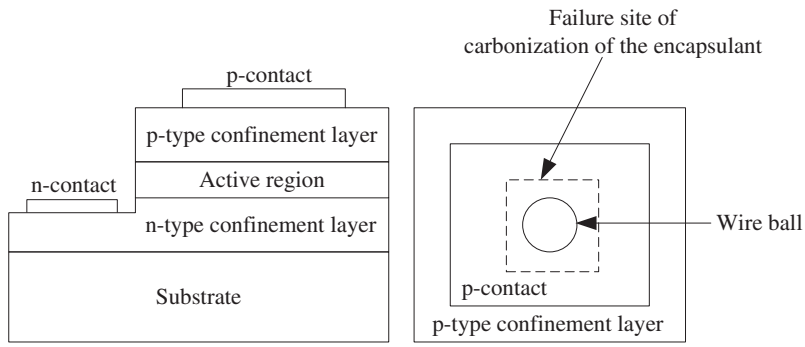

Fig. 9. Conceptual image of damaged area for carbonization of the encapsulant.

3.9. Package-related failure mechanisms: delamination

Repeated cyclic stresses can cause the material layers of LED packages to separate, causing significant loss of mechanical toughness. This causes delamination. Delamination can either occur between the die and silicone encapsulant [15], between the encapsulant and packaging lead frame [122], or between the LED die and die attach [123,124], as shown in Fig. 10.

The failure mode associated with delamination is generally decreased light output. When delamination occurs in a thermal path, the thermal resistance of the delamination layer is increased. The increased thermal resistance leads to increased junction temperature, which also affects many other failure mechanisms and ultimately reduces the life of LED packages. Delamination may also cause a permanent reduction in light output. Failure causes are thermomechanical stresses, moisture absorption, and/or interface contamination [5,98,121,122,125,126]. Interface contamination during the LED package manufacturing process can result in poor adhesion of interfaces, which can initiate delamination.

LED packages are usually molded with polymer plastic materials. Mismatching coefficients of moisture expansion (CMEs) induce hygro-mechanical stress in LED packages and cause the LED packages to swell after absorbing moisture. Different levels of swelling occur between polymeric and non-polymeric materials as well as among the polymeric materials. This differential swelling induces hygroscopic stress in the package, thus adding thermal stress at high reflow temperatures, thereby inducing delamination [127]. The moisture presence in packages can reduce interfacial adhesion strength by 40–60% and lead to delamination [121,125]. The mismatching coefficients of thermal expansion (CTEs) in LED packages also induce thermal stress during the reflow soldering process. A high temperature gradient can cause delamination between the LED die and the encapsulant, which forms a thin chip-air-silicone interface inside the LED package [121].

Kim et al. reported that the die attach quality of Au/Sn eutectic bonding with low thermal resistance was better than that of Ag paste and solder paste, which have a higher thermal resistance [124]. Die attach discontinuities result in locally increased temperatures within a package [128]. Rencz et al. analyzed and detected die attach discontinuities by structure function evaluation, which is a useful method for measuring partial thermal resistance values. The highest increase in the R_{th} value was detected when the voids were centrally located in the package [129]. Structure functions provide a map of the cumulative thermal capacitances of the heat flow path with respect to the thermal resistance from the junction to the ambient. The maximum value of the stress appears at the corner of the die and die attach. This stress led to interface delamination between the die and die attach. In most cases, the delamination begins from the corners (where the highest stress occurs) and then expands to other areas [130]. The combined effect of shear and peel stress on the delamination of an adhesive layer is experimentally known by the following relationship:

$$\left(\frac{\tau}{\sigma_f}\right)^2 + \left(\frac{\sigma}{\sigma_f}\right)^2 = 1 \tag{4}$$

where τ and σ are the shear and the peel stresses, respectively, at the interface, and σ_f is the combined failure stress for the interface [123].

Thermal transient measurements are usually performed to analyze the thermal behavior of delamination in LED packages [124,125, 131–134]. From the derivative of the structure function, the differential structure is represented as a function of the cumulative thermal resistance [135]. In both of these functions, the local peaks and valleys indicate reaching new materials or changing surface areas in the heat flow path. A peak usually indicates the middle of a new region [124]. Thermal resistance increases with the degree of delamination. Bad bonding between the chip and other parts in LED packages can increase thermal resistance by as much as fourteen times compared to a good bonding scheme across the chip surface area [136]. In the manufacturing process, a CTE mismatch between the bonding solder and bonded parts during temperature cycling causes delamination between the bonded surfaces. The curing of epoxy resins involves the repetition of shrinkage and the development of internal stress, which may also cause delamination [102].

Scanning acoustic tomography is a technique that is frequently used to detect delaminated areas in electronic packages. Driel et al. [137,138] performed scanning acoustic microscope measurements to examine the occurrence of delamination in cavity-down TBGA packages and exposed pad packages. In this technique, a sound wave is transferred through a device and any reflection (two-way) or time-delay (one-way) in the signal indicates a gap between two materials.

Nano-sized silica fillers around 25 nm to 50 nm are sometimes incorporated into encapsulant materials to minimize CTE mismatch and transmission loss as well as increase thermal conductivity [139]. Hu et al. presented thermal and mechanical analyses of

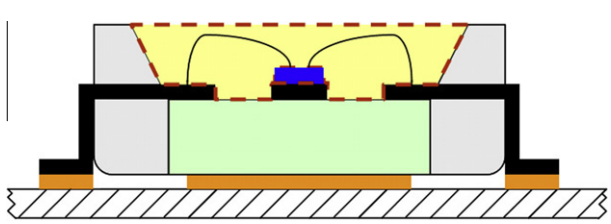

Fig. 10. Possible areas of delamination (shown by red dotted lines) caused by repeated cycle stresses in an LED. (For interpretation of the references to color in this figure legend, the reader is referred to the web version of this article.)

high power LEDs with ceramic packages [130]. The advantages of ceramic packages replacing the plastic molds include high thermal conductivity, excellent heat endurance, the ability to withstand hazardous environments, flexibility for small and thin structures, enhanced reflectivity due to advanced surface-finishing technology, less CTE mismatch with the die, and high moisture resistance [140,141]. Ceramic packages reduce thermal resistances from the junction to the ambient. As a result, ceramic packages lower delamination between interface layers in LED packages.

Proper selection of materials of LED package components with similar CTEs and CMEs is required to release thermomechanical stress and hygro-mechanical stress. Low CTE and modulus encapsulants, excellent adhesion, and CTE matching materials between the bonded surfaces are possible solutions for delamination. Also, thermal management from the die to the underlying leads of an LED package should be improved by using a large metal heat slug in the center of the bottom of LED packages or a metal core printed circuit board (MCPCB) to form a more effective conduction path.

3.10. Package-related failure mechanisms: encapsulant yellowing

LEDs are encapsulated to prevent mechanical and thermal stress shock and humidity-induced corrosion. Transparent epoxy resins are generally used as an LED encapsulant. However, epoxy resins have two disadvantages as LED encapsulants. One is that cured epoxy resins are usually hard and brittle owing to rigid cross-linked networks. The other disadvantage is that epoxy resins degrade under exposure to radiation and high temperatures, resulting in chain scission (which results in radical formation) and discoloration (due to the formation of thermo-oxidative cross-links). This is called encapsulant yellowing. Modification with silicone materials has been considered an efficient method to increase the toughness and thermal stability of transparent epoxy encapsulant resin. However, silicone compound as an LED encapsulant can have flaws, such as lower glass transition temperature (T_g), larger CTE, and poor adhesion to housing. Li et al. found that siloxane-modified LED transparent encapsulant is one possible way to improve the thermal mechanical properties, as the multifunctionality of siloxane compounds raises the crosslink density [142]. The increase of the cross-link density means that siloxane compounds improve the bond energy of the polymer chains to mitigate the chain scission.

The failure modes of encapsulant yellowing are decreased light output due to decreased encapsulant transparency and discoloration of the encapsulant. The basic causes of encapsulant yellowing are (1) prolonged exposure to short wavelength emission (blue/UV radiation), which causes photodegradation; (2) excessive junction temperature; and (3) the presence of phosphors.

Photodegradation of polymer materials usually takes place under the following conditions: (1) by increasing the molecular mobility of the polymer molecule, which is made possible by raising the temperature above T_g; and (2) the introduction of chromophores as an additive or an abnormal bond into the molecule, both of which have absorption maxima in a region where the matrix polymer has no absorption band [143]. Photodegradation depends on exposure time and the amount of radiation. Thus, even long-term exposure to visible light can cause polymer and epoxy materials to be degraded [143,144]. Down [145] reported that light-induced yellowing was grouped with four distinct types of yellowing curves: linear, autocatalytic (where the amount and rate of yellowing increase with time), auto-retardant (where yellowing proceeds at a decreasing rate), and initial bleaching followed by a linear increase in yellowing. It is well known that many epoxies can turn yellow when subjected to prolonged exposure to ultraviolet (UV) light as well as levels of blue light, since band-to-band recombination in the GaN system can produce ultraviolet radiation [118]. Discoloration results in a reduction in the transparency of the encapsulant and causes a decrease in LED light output [146]. Further, it has been demonstrated that degradation and the associated yellowing increases exponentially with exposure energy (amount of the light illuminating the encapsulant).

The thermal effects associated with excessive junction temperature also play a role in encapsulant yellowing [146,147]. Narendran et al. [144] reported that the degradation rate of 5 mm epoxy-encapsulated YAG:Ce low-power white LEDs was mainly affected by junction heat and the amount of short wavelength emissions. It was shown that the thermal effect has greater influence on yellowing than does short-wavelength radiation. Furthermore, they demonstrated that a portion of the light circulated between the phosphor layer and the reflector cup and increased the temperature, potentially causing epoxy yellowing. Yanagisawa et al. [55] also found that yellowing is not significantly affected by a high humidity test environment. Baillot et al. stated that silicone coating degradation inside the encapsulant was observed at high temperature accelerated life test conditions (30 mA/85 °C/1500 h) [148]. Barton and Osinski [149] also suggested that yellowing is related to a combination of ambient temperature and LED self-heating. Their results indicated that a temperature of around 150 °C was sufficient to change the transparency of the epoxy, causing the attenuation of the light output of LEDs.

Down [150] carried out natural dark aging on various commercially available epoxy resin adhesives that were cured at room temperature in order to discuss resistance to thermal yellowing. The extent of yellowing was monitored by measuring the absorption of the wavelengths at 380 nm and 600 nm, as shown in Eq. (5). Yellowing curves are plots of average A_t (degree of yellowing) with time (t). According to Beer's law, the absorbance is directly proportional to the thickness of the sample being measured. The results were analyzed by using the following criteria during the yellowing acceptability evaluation test: epoxy samples with an absorbance of less than 0.1 mm were always perceived as acceptable in color; samples with absorbance greater than 0.25 mm were unacceptable in color; and uncertainty in color acceptability existed from 0.1 to 0.25 mm. In practical terms, the discoloring started visibly where the yellowing curve intersects 0.1 until it reaches 0.25. However, it was considered tolerably yellow from 0.1 to 0.25, which meant it was still acceptable.

$$A_t = [A(380\ \text{nm})_t - A(600\ \text{nm})_t] \times \frac{0.1\ \text{mm}}{F} \tag{5}$$

where A_t is the degree of yellowing observed at a specific time t, and F is the average film thickness of each sample.

Although phosphors are a necessary component for producing white light, the presence of phosphors causes a decrease in reliability [147]. The phosphor is embedded inside an epoxy resin that surrounds the LED die. The phosphor converts some portion of the short wavelength light from the blue LED, and the combined blue light with the down-converted light produces the desired white light. When the phosphor is in direct contact with the die, as is the case for a phosphor-converted light emitting diode (pcLED), 60% of the phosphor emission is absorbed directly backward toward the chip. When the phosphor is not in contact with the die but away from the die, the loss is mainly from absorption by reflective surfaces and from light being trapped inside the diffused phosphor [151]. A package with lower concentration and higher phosphor thickness has a higher luminous efficacy (measured in units of lumens per watt of optical power) because the light extraction efficiency is lower with low phosphor concentrations [152]. Much research has been conducted relating different spatial phosphor distributions to reliability. Arik et al. [153] used finite element analysis to show that localized heating of the phosphor particles occurs during wavelength conversion because of low

quantum efficiency. The authors reported that as little as 3 mW heat generation on a 20 μm-diameter spherical phosphor particle can lead to excessive temperatures sufficient to degrade light output.

Thus, it is necessary to consider both photonics and thermal aspects to investigate how phosphor particles affect encapsulant yellowing. The inclusion of phosphor into an LED package must be considered based on particle size, concentration, geometry, carrier medium, and refractive index matched with the encapsulant material [151,152]. The geometry of the pcLED is usually divided into three classes: dispersed, remote, and local. A scattered photon extraction pcLED, which is a remote-type pcLED, is 61% more efficient than a conventional pcLED because the phosphor layer is separated from the die and backward-emitted rays are extracted from the sides of the optical structure inside the diffuse reflector cup of the package [151,154]. Trapping by total internal reflection (TIR) and quantum conversion (QC) loss causes optical losses inside the phosphor layer. Kim et al. used remote phosphor distribution with a diffuse reflector cup to enhance the light extraction efficiency [155]. Luo et al. [156] minimized the optical losses by utilizing a diffuse reflector cup, a remote-type phosphor layer, and a hemispherical encapsulant shape. Further, Allen and Steckl [151] found that the enhanced light extraction by internal reflection (ELiXIR) pcLED decreased the phosphor conversion loss by only 1%. ELiXIR pcLED showed a nearly ideal blue-to-white conversion obtained by internal reflection leading phosphor emissions away from the surface. This process utilizes a reflector material having high reflectivity and remotely located phosphors with a unity of quantum efficiency, a homogeneous refractive index to attenuate scattering, and a refractive index matching the encapsulant material to annihilate the total internal reflection. Li et al. reported that having fewer ZnO nanoparticles as particle fillers in a transparent epoxy matrix increases the high-visible light transparency and high-UV light shielding efficiency necessary for UV-WLEDs [157]. As can be seen in the works discussed above, enhancing light extraction efficiency was achieved by photonics and thermal consideration of the presence of phosphors in LED encapsulants.

Packaging material solutions are needed for further research on encapsulant yellowing. UV transparent encapsulant or silicone-based encapsulant will prevent photodegradation of encapsulants caused by UV radiation. Modified epoxy resins or silicone-based encapsulant and low thermal resistance substrate are useful for minimizing thermal degradation of encapsulants induced by high junction temperature between the LED die and leads. High refractive index encapsulants, efficient encapsulants and cup design, and high phosphor quantum efficiency will solve refractive index mismatch between the LED die and the encapsulant to improve light extraction efficiency.

3.11. Package-related failure mechanisms: lens cracking

The encapsulants and lens materials of LEDs are generally required to possess the characteristics of high transparency, high refractive index, chemical stability, high temperature stability, and hermeticity to enhance the extraction of light into free space as well as reliability performance [158]. High power LEDs use a plastic lens as well as an encapsulant, as shown in Fig. 11 [158]. Since standard silicone retains mechanical softness in its cured state, the silicone encapsulant is enclosed in a plastic cover that serves as a lens to give mechanical protection. The plastic lenses also serve to increase the amount of light emitted from the LEDs into free space. The failure mode of lens degradation is a number of small hairline cracks that decrease light output due to increased internal reflection in LEDs. The degradation appears due to thermo-mechanical stresses, hygro-mechanical stresses, and poor board-assembly processing.

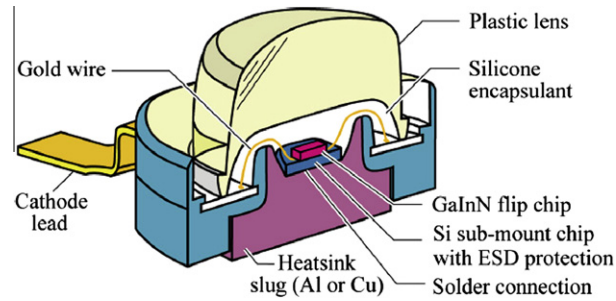

Fig. 11. Cross-sectional view of high power LED package [158] (© Cambridge University Press. Reprinted with permission.)

Lens cracking depends on the material properties of plastics. All encapsulants and lenses in LEDs are based on polymers such as epoxy resins, silicone polymers, and polymethylmethacrylate (PMMA) [1,3,14,99,158]. Hsu et al. [159] found a number of cracks introduced from thermal expansion in the center of the lens surface and on the inside of the polymer encapsulation when high power LED samples with three different lens shapes were aged at 80 °C, 100 °C, and 120 °C under a constant voltage of 3.2 V. They used LEDs with hemispherical, cylindrical, and elliptical shapes. The hemispherical lens LEDs had longer lives than the cylindrical- and elliptical-shaped plastic lenses due to a more uniform thermal dissipation along the thermal path from the LED chip to the lens [159]. It was also reported that long-term exposure to high condensing moisture caused cloudiness of the epoxy lenses in a plastic LED lamp due to hygro-mechanical stresses [100]. Philips Lumileds also reported that extreme thermal shock can crack an epoxy lens, since temperature variations in LEDs induce mechanical stress [15]. Poor PC board assembly processing causing cracked plastic domes were revealed during an electrical test when trying to bend lamps into position after soldering. The bending stresses in the lead frames were transmitted to the encapsulating epoxy, causing the epoxy to crack [100].

Further research should be focused on the selection of lens materials and efficient lens and cup design to minimize the thermomechanical stress and hygro-mechanical stress on the lens. Quality control of the lens should be improved to avoid lens cracking by implementing reliability evaluation and acceleration life tests.

3.12. Package-related failure mechanisms: phosphor thermal quenching

Phosphor thermal quenching decreases light output with the increase of the nonradiative transition probability due to thermally driven phosphorescence decay. Phosphor thermal quenching means that the efficiency of the phosphor is degraded when the temperature rises. White LEDs are usually phosphor-converted LEDs (pcLEDs) that utilize short wavelengths emitting from LED dies to excite phosphors (luminescent materials) spread over the inside of the encapsulant. Phosphors emit light with longer wavelengths and then mix with the remains of the diode light to produce the desired white color. Phosphorescence has a longer emission pathway (longer excited state lifetime) than fluorescence, as shown in Fig. 12. Phosphorescence decay is temperature dependent, while fluorescence decay is independent of temperature.

It is generally required that phosphors for white LEDs have low thermal quenching caused by a small Stokes shift to avoid changes in the chromaticity and brightness of white LEDs [160]. The types of white LEDs are class D (daylight), class N (neutral white), class W (white), class WW (warm white), and class L (incandescent light bulb). Phosphors used in white LEDs are generally divided into

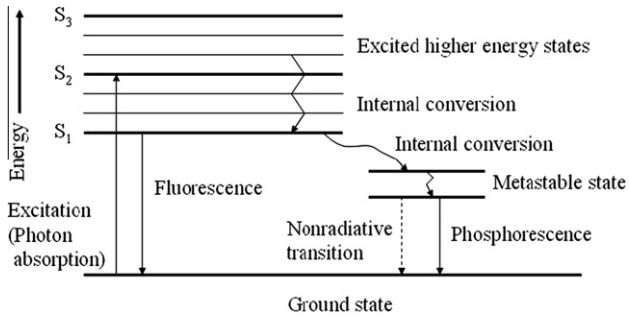

Fig. 12. Fluorescence vs. phosphorescence.

sulfides, aluminates, nitrides, and silicates. The phosphors used in LEDs are generally required to have the following characteristics: high absorption of UV or blue light; high conversion efficiency; high resistance to chemicals, oxygen, carbon dioxide, and moisture; low thermal quenching; small and uniform particle size (5–20 μm); and appropriate emission colors [161]. Most oxide-based phosphors have low absorption in the visible-light range, which means that they cannot be coupled with blue LEDs. Sulfide-based phosphors are thermally unstable and very sensitive to moisture, and they degrade significantly under ambient conditions without a protective coating layer. Xie et al. further assert that silicon-based oxynitride phosphors and nitride-based phosphors have a broad excitation band extending from the ultraviolet to the visible-light range and also the ability to strongly absorb blue-to-green light [161].

Failure modes resulting from phosphor thermal quenching include a decrease in light output, color shift, and the broadening of full width at half maximum (FWHM). The driving forces are high drive current and excessive junction temperature, which are attributed to increases in temperature of the inside of the package [98].

With increasing temperature, the nonradiative transition probability increases due to thermal activation and the release of the luminescent center through the crossing point between the excited state and the ground state [162]. This quenches the luminescence. Jia et al. demonstrated that a blue shift and spectral broadening with increasing temperature indicate temperature-dependent electron–phonon interaction [163]. The temperature dependency of phosphor thermal quenching is described in Fig. 13. Light output degradation begins to occur above a lead temperature of 80 °C (3) for high power LEDs. Upon heating, the broadening of FWHM is caused by phosphor thermal quenching ((4)–(6)). A slight blue shift of the emission band is observed for phosphors as the temperature increases. The shift of die peak wavelength to a lower energy is due to the junction temperature dependence of the energy bandgap shrinkage. The thermal quenching process was caused by either a multiple phonon relaxation process or the thermal ionization of

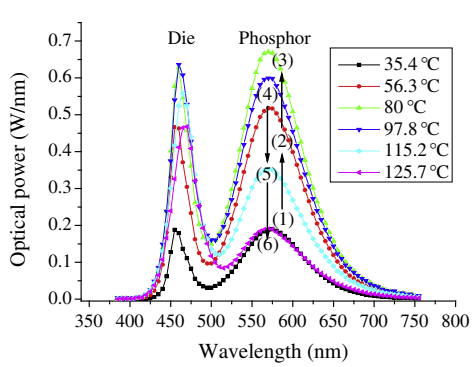

Fig. 13. Spectra change with temperature rise.

doped material as a part of a trapping mechanism that produced long persistent phosphors. Less lattice phonon energy is favored for reducing a thermal quenching process. For persistent phosphors, activators are supposed to be ionized by one photon to produce trapped electrons. The electrons need thermal energy to be ionized when the electronic excited state is below the conduction band. This process is called thermal ionization, and it requires the electron energy level to be close to the host conduction band. When thermal ionization processes exist, thermal quenching is more severe because a large number of electrons are trapped. This causes light output degradation and color change.

Xie et al. [164] used the Arrhenius equation to fit thermal quenching data in order to understand the temperature dependence of photoluminescence and determine the activation energy for thermal quenching:

$$I(T) = \frac{I_o}{1 + c * \exp\left(\frac{-E}{kT}\right)} \tag{6}$$

where I_o is the initial intensity, I(T) is the intensity at a given temperature T, c is a constant, E is the activation energy for thermal quenching, and k is Boltzmann's constant. They found the most appropriate value of the activation energy, E, to be 0.23 eV for α-sialon: Yb^{2+} and 0.20 eV for $Sr_2Si_5N_8:Eu^{2+}$.

Research for improving the reliability and design of LED packages has been conducted to minimize quantum conversion loss caused by phosphor thermal quenching. Current research is focused on solving the phosphor thermal quenching problem to enhance quantum conversion efficiency for long-term reliability by utilizing and/or developing new phosphor materials to generate white lights mixed with different colors of LED dies.

One-pcLEDs have been commercially available using a blue LED and yttrium aluminum garnet phosphors doped with Ce^{3+} ($YAG:Ce^{3+}$). One-pcLEDs produce white light by combining blue LEDs with yellow-emitting phosphors [165,166]. The conventional $YAG:Ce^{3+}$ white LED has a low color rendering index both because it lacks a red component and because it faces the problems of high thermal quenching and narrow visible range [167]. Better light quality was shown to be obtained by using a combination of a Ce^{3+} doped garnet phosphor with a red emitter [168,169]. Two-pcLEDs using a combination of red and green phosphors with blue LEDs were studied [169]. The two phosphors absorbed the blue light from the InGaN chip and converted it into green and red light, and then white light was produced by color mixing. Three-pcLEDs using a combination of red, green, and blue phosphors with UV LEDs were demonstrated by Mueller and Mueller-Mach [170]. Color mixing of red, green, and blue phosphors improved the color rendering and produced a wide range of color temperatures. Critical key values judging the quality of white light produced by pcLEDs are known as the color rendering index (CRI) and the correlated color temperature (CCT) [171]. CRI > 80 is regarded as good; in the 1970s is regarded as plain or acceptable [169,171].

Mueller-Mach et al. [171] presented a 2-pcLED based on phosphors of $Sr_2SiN_8:Eu^{2+}$ (nitridosilicates, red) and $SrSi_2O_2N_2:Eu^{2+}$ (oxonitridosilicates, green) excited by blue InGaN/GaN LEDs. These showed a wide range of CCT and good CRI with low thermal quenching. Uheda et al. [172] found that red phosphor, $CaAlSiN_3:Eu^{2+}$, is more efficient than $La_2O_2S:Eu^{3+}$ or $Ca_2Si_5N_8:Eu^{2+}$ under 460 and 405 nm excitation and is chemically stable as well, so that it produces highly efficient red-emitting phosphors excited by blue or violet LEDs. Xie et al. reported that Eu^{2+} activated Li-α-SiAlON is a good greenish yellow phosphor for pcLEDs [162,164]. Jia et al. [163] showed that phosphors of $SrMgSi_2O_6$ and $Sr_2MgSi_2O_7$ doped with Eu^{2+} were enhanced by codoping trivalent rare earth ions, such as Nd^{3+}. Li et al. [173] showed that the red emitting $Sr_2Si_5N_8:Eu^{2+}$ has a quantum efficiency of 75–80% and

very low thermal quenching up to 150 °C. Xie et al. [174] found that (oxy)nitride phosphors in the system of M–Si–Al–O–N showed high conversion efficiency of blue light, suitable emission colors, and little thermal quenching. Xie et al. further reported that a synthetic route to $Sr_2Si_5N_8:Eu^{2+}$-based red nitridosilicate phosphors showed orange-red emission and high quantum efficiency with very low thermal quenching [175]. Zeng et al. [176] demonstrated that $Ba_5SiO_4Cl_6:Eu^{2+}$ phosphors under 405 nm excitation exhibit an intense blue emission with a peak wavelength at 440 nm of more than 220% compared to conventional $BaMgAl_{10}O_{17}:Eu^{2+}$.

Further research on phosphor thermal quenching is required to enhance and maintain light extraction efficiency by optimizing the material, size, concentration, and geometry of phosphor particles to minimize temperature rise on the inside of LED packages as well as by improving the thermal design of LED packages and boards to dissipate the internal heat of LED packages through boards to the outer environment.

3.13. Package-related failure mechanisms: solder joint fatigue

LED packages are usually bonded to a ceramic (AlO), metal (MCPCB), or organic (FR4) PCB using a solder. The solder may fatigue and may lift off and/or degrade. Failure modes and their mitigation of solder joint fatigue are associated with the degradation of electrical connections (solder joints) as well as the degradation of LEDs with time. The degradation of electrical connections increases forward voltage. Thermomechanical fatigue is not a major issue for chip-on-board packaged LEDs, where the chip is directly wirebonded to the circuit board [177]. For chip-on-board packages, the critical factor for long-term reliability is degradation of the LED itself and not that of the board-level interconnects. On the other hand, in a rigid SMT submount (typically ceramic, LCP, or PMMA) type package, the solder interconnects go through stress reversals due to the CTE mismatch between the LED package and the circuit board [178], resulting in thermomechanical fatigue of the solder joint. Therefore, critical factors for long-term reliability for submount packages include thermomechanical fatigue of solder joints as well as LED degradation.

The failure mechanism could be fatigue due to deformation in response to applied mechanical stresses, cyclic creep and stress relaxation, fracture of brittle intermetallic compounds, or combinations thereof [179]. During temperature changes, shear is the primary stress on solder joints. As a result, the surfaces of solder joints slide relative to one another during thermal cycling, producing electrical transients that are typically of short duration [180]. Common failure causes of solder joint fatigue of LEDs are CTE mismatch between the package and circuit board, the geometry of the package (i.e., length scale over which stress is transmitted), solder joint material and thickness, temperature swings and dwell time, the modulus and thickness of the circuit dielectric, and the thermal resistance of the dielectric [177,181]. Chang et al. [181] stated that the reliability of the interconnects between high power LED packages and aluminum metal core printed circuit boards depends on the magnitude of the temperature swing, dwell time, electrical power of LED packages, and board design (with or without the active cooling device). The obtained simulation results showed that a high temperature swing and longer dwell time can result in shorter cycles to failure. Higher electrical power in LEDs accelerated the rate of interconnect failures at solder joints. Using an active cooling device improved the cycles to failure and made them longer than did passive cooling methods [181]. In most cases of high power LEDs, the metal heat slug located in the center of the LED package provides a mechanical connection and a thermal path to the PCB. The total effective solder joint area increases and cyclic temperature excursion decreases due to the solder joint.

The reliability of solder interconnects is influenced by environmental loads, solder material properties, and the intermetallics formed within the solder and the metal surfaces where the solder is bonded [182,183]. Osterman et al. demonstrated that the Coffin–Manson fatigue life relationship is a good model for estimating the fatigue life of solder interconnects early in the design process [184]. The Engelmaier interconnect fatigue life model was developed as an improvement upon the inelastic strain-range-based Coffin–Manson model. The Engelmaier model provides a first-order estimate of cycles to failure for solder interconnects under power and thermal cycles. However, the Engelmaier model does not consider the local CTE and the possible variations, such as thermal cycle temperature ranges and different stress levels, that a solder joint may experience. Also, the Engelmaier model does not take into account any elastic deformation and are mainly applicable to ceramic interconnect boards [185]. Intermetallic compounds are formed while metal component terminals, board pad finishes, and base board metals react. The growth of intermetallic compounds causes solder to become brittle and results in solder joint failure [183].

LED packages, high-power LED packages in particular, are nonstandard compared to other semiconductor and passive parts. For example, the metal heat slug located in the center of a high-power LED package under evaluation provides a mechanical connection and a thermal path to the aluminum MCPCB. Chang et al. [181] reported that the total effective solder joint area increased and cyclic temperature excursion decreased due to this solder joint. There are many versions of heat sink materials and shapes for which simulation tools and techniques are not well developed [186].

4. Relationship between failure causes and associated mechanisms

Based on the findings from Section 3, the causes of LED failure can be categorized as extrinsic and intrinsic causes. For example, prolonged exposure to UV, high current, poor assembly, and moisture ingress can be categorized as extrinsic causes of LED failure [187–194]. To avoid extrinsic failures, it is necessary to exercise control of environmental conditions and fine tune the manufacturing/assembly processes, which are achievable goals. However, increasing reliability by preventing intrinsic failures is more challenging, as it requires a complete understanding of the root causes of failures and their associated failure mechanisms. Hence, it is necessary to understand the causes of failure, failure modes, and associated failure mechanism(s). Based on an exhaustive literature review and research performed by CALCE, this paper lays the foundation for such an understanding. For example, delamination is one of the dominant mechanisms responsible for the failure of LEDs. One type of delamination involves the detachment of the encapsulant from the LED package. As mentioned earlier, the reduction in light output—not catastrophic failure, as in other electronic components—is the failure criterion. As can be seen in Table 2, there can be two effects on a device—thermomechanical stress and hygro-mechanical stress—that are responsible for initiating delamination, which can result in reduced light output over a period of time. Table 2 summarizes the relationships between various failure sites and the associated causes, effects on devices, failure modes, and failure mechanisms. However, new research and field experience with LEDs is necessary to develop improved understanding to further update the interrelationships shown in Table 2.

5. Challenges in LED reliability achievement due to lack of thermal standardization

When a high drive current is applied to LEDs, there is increased light output, but that typically comes with increased heat

Table 2
Failure sites, causes, effects, modes, and mechanisms of LEDs.

Failure Site	Failure Cause	Effect on Device	Failure Mode	Failure Mechanism
Semiconductor (Die)	• High Current–Induced Joule Heating	Thermomechanical Stress	Lumen Degradation, Increase in Reverse Leakage Current, Increase in Parasitic Series Resistance	Defect and Dislocation Generation and Movement
	• High Current–Induced Joule Heating • High Ambient Temperature • Poor Sawing and Grinding Process	Thermomechanical Stress	Lumen Degradation	Die Cracking
	• Poor Fabrication Process of p-n Junction • High Current–Induced Joule Heating • High Ambient Temperature	Thermal Stress	Lumen Degradation, Increase in Series Resistance and/or Forward Current	Dopant Diffusion
	• High Drive Current or High Current Density	Electrical Overstress	No Light, Short Circuit	Electromigration
Interconnects (Bond Wire, Ball, and Attachment)	• High Drive Current/ High Peak Transient Current	Electrical Overstress	No Light, Open Circuit	Electrical Overstress-Induced Bond Wire Fracture
	• Thermal Cycling Induced Deformation • Mismatch in Material Properties (e.g., CTEs, Young's Modulus)	Thermomechanical Stress	No Light, Open Circuit	Wire Ball Bond Fatigue
	• Moisture Ingress	Hygro-mechanical Stress		
	• High Drive Current or High Pulsed / Transient Current	Electrical Overstress	Lumen Degradation, Increase in Parasitic Series Resistance, Short Circuit	Electrical Contact Metallurgical Interdiffusion
	• High Temperature	Thermal Stress		
	• Poor Material Properties (e.g., poor thermal conductivity of substrate)	Thermal Resistance Increase	No Light, Open Circuit	Electrostatic Discharge
	• High Voltage (Reverse Biased Pulse)	Electrical Overstress		
Package (Encapsulant, Lens, Lead Frame, and Case)	• High Current–Induced Joule Heating • High Ambient Temperature	Electrical Overstress	Lumen Degradation	Carbonization of the Encapsulant
	• Mismatch in Material Properties (CTEs and CMEs) • Interface Contamination	Thermomechanical Stress	Lumen Degradation	Delamination
	• Moisture Ingress	Hygro-mechanical Stress		
	• Prolonged Exposure to UV	Photodegradation	Lumen Degradation, Color Change, Discoloration of the Encapsulant	Encapsulant Yellowing
	• High Drive Current Induced Joule Heating • High Ambient Temperature • Presence of Phosphor	Thermal Stress		
	• High Ambient Temperature • Poor Thermal Design	Thermomechanical Stress	Lumen Degradation	Lens Cracking
	• Moisture Ingress	Hygro-mechanical Stress		
	• High Current–Induced Joule Heating • High Ambient Temperature	Thermal Stress	Lumen Degradation, Broadening of Spectrum (Color Change)	Phosphor Thermal Quenching
	• Mismatch in Material Properties / Thermal Cycling Induced High Temperature Gradient	Mechanical Stress Cyclic Creep and Stress Relaxation Fracture of Brittle Intermetallic Compounds	Lumen Degradation, Forward Voltage Increase	Solder Joint Fatigue

generation. The light output can change as a result of the operating conditions, temperature in particular [195–201]. The level of heat generation depends on the methods of dispersing heat. For example, light output decreases with a temperature rise in LEDs, since the quantum efficiency decreases at higher temperatures, which contributes to more non-radiation recombination events in LEDs [202]. Temperature increase is also related to forward voltage drop due to the decrease of the bandgap energy of the active region of LEDs and also due to the decrease in series resistance occurring at high temperatures. The resistance decrease is due to higher acceptor activation occurring at elevated temperatures as well as the resulting higher conductivity of the p-type layer and active layers. In addition to the quantum efficiency drop, the colors of LEDs also change with increased temperature. In particular,

phosphor-converted LEDs with blue InGaN and yellow phosphors experience light output degradation, which causes shifts of blue peak wavelength and the peak energy of phosphors when the temperature of the LEDs increases. The shifts of the blue peak wavelength toward longer wavelengths having lower energy (i.e., redshifting) are due to the junction temperature dependence of the energy gap shrinkage and quantum-confined Stark effect, a process which reduces the energy of bound states in a quantum well under an applied electric field [203]. On the contrary, the shifts of the blue peak wavelength toward shorter wavelengths having higher energy (i.e., blue shifting) are due to band filling, a process which results from the injection of holes via tunneling into an empty impurity band and vacant valence band [204]. The peak energy shifts of the phosphors are due to phosphor thermal quenching. To sum up, many important reliability-related features of LEDs are functions of temperature.

The long-term stability and lifetime of LEDs are typically judged on the basis of measured light output. The measured light output mostly depends on the junction temperature. Hence, the correctness of light output measurements is dependent on the temperature stability of the light output measurement setup and on the accuracy of the temperature measurement. There are uncertainties associated with the prediction of the junction temperature because there are only indirect ways of measuring and evaluating temperatures from reference points to the junction temperature. Long-term stability analyses of LEDs need to demonstrate that the thermal conditions of the LEDs have not changed during the entire aging/testing process in order to enable correct correlation between light output characteristics and $R\mathrm{th}_{\mathrm{J\text{-}A}}$ (thermal resistance between LED junction and ambient). Little information has been published about how the light output measurements in reliability studies are performed, but it is suspected that $R\mathrm{th}_{\mathrm{J\text{-}A}}$ of LEDs during aging test measurements is often uncontrolled and changes over time. As a consequence, some of the reported light output variations could be attributed to $R\mathrm{th}_{\mathrm{J\text{-}A}}$ variations of the test setup. One way to prevent this is to eliminate the potential changes in $R\mathrm{th}_{\mathrm{J\text{-}A}}$ by ensuring that all light output characteristics are presented as a function of the real junction temperature. The only way that the reliability data provided by different vendors can be assured is by standardizing all relevant measurements and definitions.

Besides the standardization of reliability-related tests, an important source of information for a designer is the published data in the data sheets, especially thermal data such as junction-to-ambient and junction-to-case thermal resistances. The designer needs these data to ensure that the maximum allowable temperatures prescribed by the vendors are not exceeded. It is necessary for these data to be standardized, because lower thermal resistance is a major selection criterion. Lasance and Poppe [205–208] and Poppe et al. [209] discussed the need for more sophisticated thermal characterization and standardization of LEDs and LED-based products. The reason is that progress in these fields has not kept pace with the exponential growth in applications. This situation is becoming a serious problem for leading manufacturers who are focusing on a sustainable business for the future and are willing to publish reliable thermal data. Unfortunately, due to the lack of globally accepted standards, manufacturers can publish whatever they want. The lack of standards also becomes a problem for the experienced user because the thermal data that are published are often of limited use in practice when accuracy is at stake, and accuracy is needed for estimation of expected performance and lifetime. Remarkably, the situation is not much different from the one that the IC (integrated circuit)-world was facing almost 20 years ago [209–214]. Around 1990 it became clear that thermal characterization of IC packages was problematic. Manufacturers all over the world were using different standards. Even within a single manufacturer, intolerable differences showed up. To solve the thermal characterization problems, manufacturers must publish thermal data in such a way that the end-user can use this data. End-users are responsible for the specifications of the thermal environment to which the LEDs are exposed. Provided that the manufacturers want to cooperate, it would be easy to apply the standard protocols used by the IC business.

In addition to standardization itself and suggestions for improved test setups, Poppe and Lasance discussed [205–208] the role of thermal characterization, the definition of thermal resistance, the different goals of manufacturers and system designers, the similarities and differences between LED and IC thermal characterization, the drawbacks of the current thermal data in data sheets, and an overview of the questions that an LED thermal standardization body should address.

6. Summary and recommendations

The conventional way to predict the lifetime of LEDs employs the Arrhenius model to extrapolate test results at high temperature to expected operating temperatures. The Arrhenius model as given in Eq. (1) is not adequate to represent the failures of LEDs. Light output degradation is the major failure mode of LEDs, and it results from hygro-mechanical and electrical stresses in addition to thermal stresses. A more realistic method of LED lifetime estimation is required that reflects total consideration of temperature, the level of forward current, relative humidity, mechanical stress, and materials. The coverage of this paper will help both to develop reliable product design for industry and provide researchers guidelines for addressing issues related to LED reliability.

The literature available on the testing of LEDs shows that extensive accelerated tests have been performed not only for academic interest but also by agencies dealing with commercial aspects of LEDs. Reliability tests have been used to claim that the typical life of LEDs can be expected to range from 3000 h for LEDs operating in harsh environments (in terms of high current, high temperature, and high humidity) to 50,000 h in benign environments. For example, LEDs running with the absolute maximum rating of current at high temperature over 85 °C and high humidity over 85% might have the worst lifetime among different usage conditions. The higher estimate for LED life is for benign conditions below room temperature and below typical operating currents. The overall reliability of LED packages is related to interconnect failures, semiconductor failures, and package failures. Interconnect failures are responsible for broken bond wires and lifted balls, electrical metallurgical interdiffusion, and electrostatic discharge. LED semiconductor failures are manifested as die cracking, defect and dislocation generation and movement, dopant diffusion, and electromigration. Package failures involve mechanical interaction with LED chips, die adhesives, heat slugs, lead frames, and encapsulants. The failure mechanisms responsible for package failures include carbonization of the encapsulant, delamination, encapsulant yellowing, phosphor thermal quenching, and lens degradation.

It is necessary to control die cracking in LEDs by fine-tuning the coefficients of thermal expansion between the substrate and epitaxial layers. The growth of the optimal medium layer between the substrate and the epitaxial layer is a key technology to prevent the die cracking. ESD resistance can be improved by employing a correctly rated Zener diode reverse-biased in parallel with the LED and by incorporating an internal GaN Schottky diode into nitride-based LEDs. Inverse-parallel shunt GaN ESD diodes also improve the ESD reliability of GaN-based LEDs. It is imperative that all vendors use globally accepted thermal standards to determine junction temperature to enable a fair comparison between different products, including agreed upon definitions of power and thermal resistance.

An improved understanding of the root causes responsible for failures in LEDs with respect to improving material properties and fabrication technology must be developed. A deeper understanding of various process variables and associated environments critical for LED quality must form part of LED reliability research. We identified the following areas for research and development to ensure that the demand for high reliability and high performance LEDs can be met by industry while meeting the Green promises.

Further research on defect and dislocation generation and motion requires improved structural and material design of LED dies and better internal thermal management handling of thermal resistance from the junction of the LED die to the package. This will reduce the formation of crystal defects and dislocation movement caused by high-current-induced thermal effects and high ambient temperature. Proper thermal management and innovative package designs are required to solve the electromigration problem. The thermal conductivities of interface materials, which account for a large portion of the thermal resistance, should be improved to prevent electromigration. In addition, low thermal conductivity control at high ambient temperatures must be taken into account in the design process.

The bonding process should be optimized by controlling wire type, pad metallization, and device configurations. Targeted bonding tests have to be performed by varying the bonding parameters, such as clamping force, power, and time-matching bond-pull strength, to extract optimum bonding conditions. The chip damage under the bonding strength condition should also be minimized.

There is a need to develop new materials for LED package components with similar CTEs and CMEs to release thermomechanical stress and hygro-mechanical stress. Low CTE and modulus of encapsulants, excellent adhesion, and CTE matching materials between the bonded surfaces are possible solutions for delamination. Also, thermal management from the die to the underlying leads of an LED package should be improved by using a metal heat slug in the center of the bottom of LED packages or by using metal core printed circuit boards (MCPCBs) to perform more effective conduction path.

Packaging material solutions are needed for further research on encapsulant yellowing. UV transparent encapsulants or silicone-based encapsulants will prevent photodegradation of encapsulants caused by UV radiation. Modified epoxy resins or silicone-based encapsulants and low thermal resistance substrates are useful for minimizing the thermal degradation of encapsulants induced by high junction temperature between the LED die and leads. A high refractive index encapsulant, efficient encapsulant and cup design, and high phosphor quantum efficiency will address the refractive index mismatch between the LED die and the encapsulant to improve light extraction efficiency.

Focused research should be conducted on the selection of lens materials and efficient lens and cup design to minimize thermomechanical stress and hygro-mechanical stress. There is also the need to improve quality control by reliability evaluation and accelerated life tests to avoid lens cracking. Prevention on phosphor thermal quenching is required to enhance and maintain light extraction efficiency by optimizing the materials, size, concentration, and geometry of phosphor particles to minimize the temperature rise on the inside of LED packages. It is also necessary to improve the thermal design of LED packages and boards to dissipate the internal heat of LED packages through boards to the outside environment so as to prevent phosphor thermal quenching.

Lifetime prediction methods are required for the observed failure modes of LEDs. Numerical prediction techniques will better facilitate our understanding of them. To achieve the goal of remaining useful life estimation in operation, prognostics and health management (PHM) techniques are necessary. In-situ monitoring can explain how the maintenance of each test parameter changes in real-time without increasing the time and number of test operators.

Failure analysis of LEDs has been performed through conventional microelectronics failure analysis approaches and off-line analysis techniques. There is a need to develop advanced failure analysis techniques for LEDs. This includes, for example, non-destructive analyses of semiconductors, interconnects, and package failures of LEDs, and in-line (event) detection methods for lumen degradation.

Cooperation between thermal, electrical, and optical standards bodies and professional societies is required to arrive at globally accepted thermal standards to measure junction and reference temperatures to ensure a fair comparison of published performance and reliability data. Since end users require the total reliability of final products, reliability research of LED packages has to be expanded to the reliability study of complete LED-based systems, including luminaires and electronics. Failure mechanisms that lead to catastrophic failure (i.e., die cracking, electromigration, electrical overstress-induced-bond wire fracture, wire ball bond fatigue, electrostatic discharge, and carbonization of the encapsulant) as well as degradation mechanisms (defect and dislocation generation and movement, dopant diffusion, electrical contact metallurgical interdiffusion, delamination, encapsulant yellowing, lens cracking, phosphor thermal quenching, and solder joint fatigue) should be considered for system-level life prediction that can accommodate long-term regional operating conditions.

There is a need to acquire knowledge of the life cycle loading conditions, geometry, and material properties of LEDs to identify potential failure mechanisms and estimate their remaining useful life. The physics-of-failure (PoF) approach considers qualification to be an integral part of the design and development process and involves identifying root causes of failure and developing qualification tests that focus on those particular issues. PHM-based-qualification combined with the PoF qualification process can enhance the evaluation of LED reliability in its actual life-cycle conditions to assess degradation, detect early failures of LEDs, estimate the lifetime of LEDs, and mitigate LED-based-product risks. The determination of aging test conditions that are improved with PHM-based-qualification enables better representation of the final usage conditions of LEDs.

Acknowledgments

The authors would like to thank the more than 100 companies and organizations that support research activities at the Center for Advanced Life Cycle Engineering at the University of Maryland annually, specifically the CALCE Prognostics and Health Management Group. We thank Prof. Bongtae Han for his review and Mark Zimmerman for copyediting. We are also grateful to Dr. Clemens Lasance, Dr. Andras Poppe, and Dr. Willem van Driel for their critical review and comments.

References

[1] Krames MR, Shchekin OB, Mueller-Mach R, Mueller GO, Zhou L, Harbers G, et al. Status and future of high-power light-emitting diodes for solid-state lighting. J Disp Technol 2007;3:160–75.
[2] Steigerwald DA, Bhat JC, Collins D, Fletcher RM, Holcomb MO, Ludowise MJ, et al. Illumination with solid state lighting technology. IEEE J Sel Top Quant Electron 2002;2:310–20.
[3] Steranka FM, Bhat J, Collins D, Cook L, Craford MG, Fletcher R, et al. High power LEDs – technology status and market applications. Phys Status Solidi A 2002;194:380–8.
[4] Schubert EF, Kim JK, Luo H, Xi J-Q. Solid-state lighting-a benevolent technology. Rep Prog Phys 2006;69:3069–99.
[5] Aoyama Y, Yachi T. An LED module array system designed for streetlight use. IEEE Energy 2008;2030:1–5.

[6] Vittori R, Scaburri A. New solid state technologies and light emission diodes as a mean of control and lighting source applicable to explosion proof equipment, with the scope to reduce maintenance, to limit the risk of bad maintenance and to expand the plants' life. PCIC Europe 2009:193–8.
[7] King M. Characteristics of high brightness LEDs. Electronic design online conference series, session 5; June 22nd, 2010. p. 1–16.
[8] Schubert EF. Light-emitting diodes. 2nd ed. New York: Cambridge University Press; 2006 [chapter 18].
[9] Huang M-S, Hung C-C, Fang Y-C, Lai W-C, Chen Y-L. Optical design and optimization of light emitting diode automotive head light with digital micromirror device light emitting diode. Optik – Int J Light Electron Opt 2009:1–9.
[10] Lee SWR, Lau CH, Chan SP, Ma KY, NG MH, NG YW, et al. Development and prototyping of a HB-LED array module for indoor solid state lighting. Proc HDP 2006:141–5.
[11] Peon R, Doluweera G, Platonova I, Irvine-Halliday D, Irvine-Halliday G. Solid state lighting for the developing world – the only solution. Optics & photonics 2005, proceedings of SPIE 5941; 2005. p. 109–23.
[12] Pinto RA, Cosetin MR, da Silva MF, Denardin GW, Fraytag J, Campos A, et al. Compact emergency lamp using power LEDs. 35th annual conference of IEEE IECON 09; 2009. p. 3494–9.
[13] Shibata S-I, Oyabu T, Kimura H. Bioelectric potential characteristic of pothos under light emitting diode. ICCAS-SICE 2009:4663–8.
[14] Wipiejewski T, Moriarty T, Hung V, Doyle P, Duggan G, Barrow D, et al. Gigabits in the home with plugless plastic optical fiber (POF) interconnects. 2nd ESTC; 2008. p. 1263–6.
[15] Lumileds. Luxeon reliability, Reliability Datasheet RD25, Philips Lumileds; 2006.
[16] Chang YN, Hung CC, Tung SC. Auto mixed light for RGB LED backlight module, ISIE 2009. IEEE international symposium; 2009. p. 864–9.
[17] Chang SW. LED lighting: high efficiency and environmental benefit, vol. 206. In: Samsung Economic Research Institute Economic Focus; 2008. p. 1–10.
[18] Narendran N, Deng L, Pysar RM, Gu Y, Yu H. Performance characteristics of high-power light-emitting diodes. 3rd international conference on solid state lighting, proceedings of SPIE 5187; 2004. p. 267–75.
[19] IES (Illuminating Engineering Society), IES LM-80-08. Approved method: measuring lumen maintenance of LED light sources; 2008.
[20] Deshayes Y, Bechou L, Verdier F, Danto Y. Long-term reliability prediction of 935nm LEDs using failure laws and low acceleration factor ageing tests. Qual Reliab Eng Int 2005;21:571–94.
[21] Trevisanello L, Meneghini M, Mura G, Vanzi M, Pavesi M, Meneghesso G, et al. Accelerated life test of high brightness light emitting diodes. IEEE Trans Dev Mater Reliab 2008;8:304–11.
[22] Deshayes Y, Bord I, Barreau G, Aiche M, Moretto PH, Bechou L, et al. Selective activation of failure mechanisms in packaged double-heterostructure light emitting diodes using controlled neutron energy irradiation. Microelectron Reliab 2008;48:1354–60.
[23] Cree. Cree Xlamp XR family LED reliability, CLD-AP06 Rev. 7, Cree, Inc.; 2009.
[24] Nichia. Specifications for Nichia chip type white LED model: NCSW119T-H3, Nichia STS-DA1-0990A, Nichia Corporation; 2009.
[25] Jeong J-S, Jung J-K, Park S-D. Reliability improvement of InGaN LED backlight module by accelerated life test (ALT) and screen policy of potential leakage LED. Microelectron Reliab 2008;48:1216–20.
[26] Polavarapu I, Okogbaa G. An interval estimate of mean-time-to-failure for a product with reciprocal weibull degradation failure rate. Proceedings of reliability and maintainability symposium; 2005. p. 261–5.
[27] Peng C-Y, Tseng S-T. Mis-specification analysis of linear degradation models. IEEE Trans Reliab 2009;58:444–55.
[28] Vazquez M, Nunez N, Nogueira E, Borreguero A. Degradation of AlInGaP red LEDs under drive current and temperature accelerated life tests. Microelectron Reliab 2010;50:1559–62.
[29] Lasance CJM. Recent progress in compact thermal models. 19th IEEE SEMI-THERM symposium; 2003. p. 290–9.
[30] Hwang N. Failure analysis matrix of light emitting diodes for general lighting applications, IPFA 2008. 15th international symposium; 2008. p. 1–4.
[31] Hu Q, Zane R. LED drive circuit with series input connected converter cells operating in continuous conduction mode, APEC 2009. 24th annual IEEE; 2009. p. 1511–7.
[32] Christensen A, Graham S. Thermal effects in packaging high power light emitting diode arrays. Appl Therm Eng 2009;29:364–71.
[33] Li Q, Kececioglu DB. Design of an optimal plan for an accelerated degradation test: a case study. Int J Qual Reliab Manage 2006;23:426–40.
[34] Nogueira E, Vazquez M, Nunez N. Evaluation of AlGaInP LEDs reliability based on accelerated tests. Microelectron Reliab 2009;49:1240–3.
[35] Kang J-M, Kim J-W, Choi J-H, Kim D-H, Kwon H-K. Life-time estimation of high-power blue light-emitting diode chips. Microelectron Reliab 2009;49:1231–5.
[36] Cheng T, Luo X, Huang S, Liu S. Thermal analysis and optimization of multiple LED packaging based on a general analytical solution. Int J Therm Sci 2010;49:196–201.
[37] Molnar G, Nagy G, Szucs Z. A novel procedure and device to allow comprehensive characterization of power LEDs over a wide range of temperature. TERMINIC 2008:89–92.
[38] Szekely V, Somlay G, Szabo PG, Rencz M. Design of a static TIM tester. THERMINIC 2008:132–6.
[39] Linderman R, Brunschwiler T, Smith B, Michel B. High-performance thermal interface technology overviews, THERMINIC 2007. 13th international workshop; 2007. p. 129–34.
[40] Horng R-H, Hsiao H-Y, Chiang C-C, Wuu D-S, Tsai Y-L, Lin H-I. Novel device design for high-power InGaN/sapphire LEDs using copper heat spreader with reflector. IEEE J Sel Top Quant Electron 2009;15:1281–6.
[41] Yu JH, Oepts W, Konijn H. PC board thermal management of high power LEDs. 24th annual IEEE semi-therm; 2008. p. 63–7.
[42] Chang H, Lai Y-S. Novel AC driver and protection circuits with dimming control for light emitting diodes. IEEE 42nd IAS annual meeting; 2007. p. 696–700.
[43] Cassanelli G, Mura G, Fantini F, Vanzi M. Failure analysis of high power white LEDs, MIEL 2008. 26th international conference; 2008. p. 255–7.
[44] Doshi M, Zane R. Reconfigurable and fault tolerant digital phase shifted modulator for luminance control of LED light sources. IEEE PESC; 2008. p. 4185–91.
[45] Hu Q, Zane R. LED drive circuit with series input connected converter cells operating in continuous conduction mode. 24th annual IEEE applied power electronics conference and exposition; 2009. p. 1511–7.
[46] Patterson J, Zane R. Series input modular architecture for driving multiple LEDs. IEEE power electronics specialists conference; 2008. p. 2650–6.
[47] Subramanian K. LED color-temperature control. Electronic design online conference series, session 2; June 22nd, 2010. p. 1–19.
[48] Ice C. Digitally controlled LED lighting systems. Electronic design online conference series, session 3; June 22nd, 2010. p. 1–28.
[49] J. Denicholas, Using analog semiconductor technologies in solid state lighting applications, Electronic Design Online Conference Series, session 4, Jun 22nd, 2010, pp. 1-46.
[50] Yanagisawa T. The degradation of GaAlAs red light-emitting diodes under continuous and low-speed pulse operations. Microelectron Reliab 1998;38:1627–30.
[51] Hoang T, LeMinh P, Holleman J, Schmitz J. The effect of dislocation loops on the light emission of silicon LEDs. 35th European solid-state device research conference; 2005. p. 359–62.
[52] Lu G, Yang S, Huang Y. Analysis on failure modes and mechanisms of LED. 8th ICRMS; 2009. p. 1237–41.
[53] Tharian J. Degradation- and failure mode analysis of III-V nitride devices, IPFA 2007. 14th international symposium; 2007. p. 284–7.
[54] Uddin A, Wei AC, Andersson TG. Study of degradation mechanism of blue light emitting diodes. Thin Solid Films 2005;483:378–81.
[55] Yanagisawa T, Kojima T. Long-term accelerated current operation of white light-emitting diodes. J Lumin 2005;114:39–42.
[56] Meneghesso G, Levada S, Zanoni E, Podda S, Mura G, Vanzi M, et al. Failure modes and mechanisms of DC-aged GaN LEDs. Phys Status Solidi A 2002;194:389–92.
[57] Meneghesso G, Levada S, Pierobon R, Rampazzo F, Zanoni E, Cavallini A, et al. Degradation mechanisms of GaN-based LEDs after accelerated DC current aging. IEDM 02 Digest Int 2002:103–6.
[58] Pavesi M, Rossi F, Zanoni E. Effects of extreme DC-ageing and electron-beam irradiation in InGaN/ AlGaN/ GaN light-emitting diodes. Semiconduct Sci Technol 2006;21:138–43.
[59] Ott M. Capabilities and reliability of LEDs and laser diodes. International NASA Parts and Packaging Publication; 1996. p. 1–7.
[60] Chuang S, Ishibashi A, Kijima S, Nakayama N, Ukita M, Taniguchi S. Kinetic model for degradation of light-emitting diodes. IEEE J Quant Electron 1997;33:970–9.
[61] Shah JM, Li Y-L, Gessmann T, Schubert EF. Experimental analysis and theoretical model for anomalously high ideal factors (n»2.0) in AlGaN/GaN p-n junction diodes. J Appl Phys 2003;94:2627–30.
[62] Sugiura L. Comparison of degradation caused by dislocation motion in compound semiconductor light-emitting devices. Appl Phys Lett 1997;70:1317–9.
[63] Sugiura L. Dislocation motion in GaN light-emitting devices and its effect on device lifetime. J Appl Phys 1997;81:1633–8.
[64] Ueda O. Reliability issues in III-V compound semiconductor devices: optical devices and GaAs-based HBTs. Microelectron Reliab 1999;39: 1839–55.
[65] Fukuda M. Laser and LED reliability update. J Lightwave Technol 1988;6:1488–95.
[66] Wang WK, Wuu DS, Lin SH, Huang SY, Wen KS, Horng RH. Growth and characterization of InGaN-based light-emitting diodes on patterned sapphire substrates. J Phys Chem Solids 2008;69:714–8.
[67] Ferenczi G. Reliability of LED's; are the accelerated ageing tests reliable? Electrocompon Sci Technol 1982;9:239–42.
[68] Rossi F, Pavesi M, Meneghini M, Salviati G, Manfredi M, Meneghesso G, et al. Influence of short-term low current DC aging on the electrical and optical properties of InGaN blue light-emitting diodes. J Appl Phys 2006;99:0531041–47.
[69] Arnold J. When the light go out: LED failure mode and mechanisms. DfR solutions; 2004. p. 1–4.
[70] Khan A, Hwang S, Lowder J. Reliability issues in AlGaN based deep ultraviolet light emitting diodes. IEEE 47th annual international reliability physics symposium; 2009. p. 89–93.
[71] Pan C, Lee C, Liu J, Chen G, Chyi J. Luminescence efficiency of InGaN multiple-quantum-well ultraviolet light-emitting diodes. Appl Phys Lett 2004;84:5249–51.

[72] Pavesi M, Manfredi M, Salviati G, Armani N, Rossi F, Meneghesso G, et al. Optical evidence of an electrothermal degradation of InGaN-based light-emitting diodes during electrical stress. Appl Phys Lett 2004;84:3403–5.
[73] Pavesi M, Manfredi M, Rossi F, Meneghini M, Zanoni E, Zehnder U, et al. Temperature dependence of the electrical activity of localized defects in InGaN-based light emitting diodes. Appl Phys Lett 2006;89:0419171–73.
[74] Cao XA, Sandvik PM, LeBoeuf SF, Arthur SD. Defect generation in InGaN/GaN light-emitting diodes under forward and reverse electrical stresses. Microelectron Reliab 2003;43:1987–91.
[75] Barton DL, Osinski M, Perlin P, Helms CJ, Berg NH. Life tests and failure mechanisms of GaN/AlGaN/InGaN light emitting diodes. IEEE 35th annual proceedings of reliability physics symposium; 1997. p. 276–81.
[76] Wu JD, Huang CY, Liao CC. Fracture strength characterization and failure analysis of silicon dies. Microelectron Reliab 2003;43:269–77.
[77] Iksan H, Lin K-L, Hsieh J. Fracture analysis on die crack failure. IMAPS Taiwan; 2001. p. 35–43.
[78] Chen CH, Tsai MY, Tang JY, Tsai WL, Chen TJ. Determination of LED die strength. International conference of EMAP; 2007. p. 1–6.
[79] Nakamura S, Mukai T, Senoh M, Iwasa N. Thermal annealing effects on p-type Mg-doped GaN films. Jpn J Appl Phys 1992;31:L139–42.
[80] Hull BA, Mohney SE, Venugopalan HS, Ramer JC. Influence of oxygen on the activation of p-type GaN. Appl Phys Lett 2000;76:2271–3.
[81] Brandt O, Yang H, Kostial H, Ploog KH. High p-type conductivity in cubic GaN/GaAs (113)A by using Be as the acceptor and O as the codopant. Appl Phys Lett 1996;69:2707–9.
[82] Kim KS, Han MS, Yang GM, Youn CJ, Lee HJ, Cho HK, et al. Codoping characteristics of Zn with Mg in GaN. Appl Phys Lett 2000;77:1123–5.
[83] Zhang X, Chua S-J, Li P, Chong K-B, Wang W. Improved Mg-doped GaN films grown over a multilayered buffer. Appl Phys Lett 2000;73:1772–4.
[84] Kim D-J, Kim H-M, Han M-G, Moon Y-T, Lee S, Park S-J. J Vac Sci Technol B 2003;21:641–4.
[85] Jang J-S, Park S-J, Seong T-Y. Metallization scheme for highly low-resistance, transparent, and thermally stable ohmic contacts to p-GaN. Appl Phys Lett 2000;76:2898–900.
[86] Khanna R, Stafford L, Voss LF, Pearton SJ, Wang HT, Anderson T, et al. Aging and stability of GaN high electron mobility transistors and light-emitting diodes with TiB2- and Ir-based contacts. IEEE Trans Dev Mater Reliab 2008;8:272–6.
[87] Zhu Q-S, Nagai H, Kawaguchi Y, Hiramatsu K, Sawaki N. Effect of thermal annealing on hole trap levels in Mg-doped GaN grown by metalorganic vapor phase epitaxy. J Vac Sci Technol A: Vac Surf Films 2000;18:261–7.
[88] Kohler K, Stephan T, Perona A, Wiegert J, Maier M, Kunzer M, et al. Control of the Mg doping profile in III-N light-emitting diodes and its effect on the electroluminescence efficiency. J Appl Phys 2005;97:1049141–44.
[89] Kwon M-K, Park I-K, Kim J-Y, Kim J-O, Kim B, Park S-J. Gradient doping of Mg in p-type GaN for high efficiency InGaN-GaN ultraviolet light-emitting diode. IEEE Photonics Technol Lett 2007;19:1880–2.
[90] Altieri-Weimar P, Jaeger A, Lutz T, Stauss P, Streubel K, Thonke K, et al. Influence of doping on the reliability of AlGaInP LEDs. J Mater Sci: Mater Electron 2008;19:S338–41.
[91] Meneghesso G, Levada S, Zanoni E. Failure mechanisms of GaN-based LEDs related with instabilities in doping profile and deep levels. IEEE forty second annual international reliability physics symposium; 2004. p. 474–8.
[92] Kozodoy P, DenBaars SP, Mishra UK. Depletion region effects in Mg-doped GaN. J Appl Phys 2000;87:770–5.
[93] Meneghini M, Trevisanello L-R, Levada S, Meneghesso G, Tamiazzo G, Zanoni E, et al. Failure mechanisms of gallium nitride LEDs related with passivation. IEEE IEDM Technical Digest 2005:1009–12.
[94] Hwang N, Naidu PSR, Trigg A. Failure analysis of plastic packaged optocoupler light emitting diodes. 5th conference EPTC; 2003. p. 346–9.
[95] Kim H, Yang H, Huh C, Kim S-W, Park S-J, Hwang H. Electromigration-induced failure of GaN multi-quantum well light emitting diode. Electron Lett 2000;36:908–10.
[96] Haque S, Steigerwald D, Rudaz S, Steward B, Bhat J, Collins D, et al. Packaging challenges of high power LEDs for solid state lighting. IMAPS Boston, MA; 2003. p. 1–5.
[97] Barton DL, Zeller J, Phillips BS, Chiu P-C, Askar S, Lee D-S, et al. Degradation of blue AlGaN/InGaN/GaN LEDs subjected to high current pulses. 33rd annual proceedings of ieee international reliability physics symposium; 1995. p. 191–9.
[98] Barton DL, Osinski M, Perlin P, Eliseev PG, Lee J. Single-quantum well InGaN green light emitting diode degradation under high electrical stress. Microelectron Reliab 1999;39:1219–27.
[99] Song BM, Han B. Reliability guidelines of high power LED. 2008 CALCE EPS consortium report. Project No. C08-26; 2008. p. 1–11.
[100] Hewlett Packard. Reliability of precision optical performance AlInGaP LED lamps in traffic signals and variable message sings. Application Brief I-004; 1997.
[101] Wu F, Zhao W, Yang S, Zhang C. Failure modes and failure analysis of white LEDs. 9th ICEMI 09; 2009. p. 4-978–4-981.
[102] Shammas NYA. Present problems of power module packaging technology. Microelectron Reliab 2003;43:519–27.
[103] Damann M, Leuther A, Benkhelifa F, Feltgen T, Jantz W. Reliability and degradation mechanism of AlGaAs/InGaAs and InAlAs/InGaAs HEMTs. Phys Status Solidi A 2003;195:81–6.
[104] Meneghesso G, Crosato C, Garat F, Martines G, Paccagnella A, Zanoni E. Failure mechanisms of schottky gate contact degradation and deep traps creations in AlGaAs/InGaAs PM-HEMTs submitted to accelerated life tests. Microelectron Reliab 1998;38:1227–32.
[105] Mizuishi K, Kurano H, Sato H, Kodera H. Degradation mechanisms of GaAs MESFETs. IEEE Trans Electron Dev 1979;ED-26:1008–14.
[106] Meneghini M, Trevisanello L-R, Zehnder U, Meneghesso G, Zanoni E. Reversible degradation of ohmic contacts on p-GaN for application in high-brightness LEDs. IEEE Trans Electron Dev 2007;54:3245–51.
[107] Jacob P, Kunz A, Nicoletti G. Reliability and wearout characterisation of LEDs. Microelectron Reliab 2006;46:1711–4.
[108] Chang SJ, Chen CH, Su YK, Sheu JK, Lai WC, Tsai JM, et al. Improved ESD protection by combining InGaN-GaN MQW LEDs with GaN schottky diodes. IEEE Electron Dev Lett 2003;24:129–31.
[109] O'Mahony D, Zimmerman W, Steffen S, Hilgarth J, Maaskant P, Ginige R, et al. Free-standing gallium nitride schottky diode characteristics and stability in a high-temperature environment. Semiconduct Sci Technol 2009;24:1–8.
[110] Shei S-C, Sheu J-K, Shen C-F. Improved reliability and ESD characteristics of flip-chip GaN-based LEDs with internal inverse-parallel protection diodes. IEEE Electron Dev Lett 2007;28:346–9.
[111] Su YK, Chang SJ, Wei SC, Chen S-M, Li W-L. ESD engineering of nitride-based LEDs. IEEE Trans Dev Mater Reliab 2005;5:277–81.
[112] Tsai CM, Sheu JK, Wang PT, Lai WC, Shei SC, Chang SJ, et al. High efficiency and improved ESD characteristics of GaN-based LEDs with naturally textured surface grown by MOCVD. IEEE Photonics Technol Lett 2006;18:1213–5.
[113] Zhang J-M, Zou D-S, Xu C, Zhu Y-X, Liang T, Da X-L, et al. High power and high reliability GaN/ InGaN flip-chip light-emitting diodes. Chin Phys 2007;16:1135–9.
[114] Meneghesso G, Chini A, Maschietto A, Zanoni E, Malberti P, Ciappa M. Electrostatic discharge and electrical overstress on GaN/InGaN light emitting diodes. Electr Overstress/Electrostatic Discharge Symp 2001:247–52.
[115] Wen TC, Chang SJ, Su YK, Wu LW, Kuo CH, Hsu YP, et al. Improved ESD reliability by using a modulation doped $Al_{0.12}$ $Ga_{0.88}$ N/GaN superlattice in nitride-based LED. International semiconductor device research symposium; 2003. p. 77–8.
[116] McCluskey P, Mensah K, O'Connor C, Lilie F, Gallo A, Pink J. Reliability of commercial plastic encapsulated microelectronics at temperatures from 125 °C to 300 °C. Proc HITEN 1999; 1999. p. 155–62.
[117] McCluskey P, Mensah K, O'Connor C, Gallo A. Reliable use of commercial technology in high temperature environments. Microelectron Reliab 2000;40:1671–8.
[118] Meneghesso G, Leveda S, Zanoni E, Scamarcio G, Mura G, Podda S, et al. Reliability of visible GaN LEDs in plastic package. Microelectron Reliab 2003;43:1737–42.
[119] Meneghini M, Trevisanello L, Sanna C, Mura G, Vanzi M, Meneghesso G, et al. High temperature electro-optical degradation of InGaN/GaN HBLEDs. Microelectron Reliab 2007;47:1625–9.
[120] Wu F, Wu Y, An B, Wu F. Analysis of dark stain on chip surface of high-power LED. 7th ICEPT'06; 2006. p. 1–4.
[121] Zhou L, An B, Wu Y, Liu S. Analysis of delamination and darkening in high power LED packaging, IPFA 2009. 16th IEEE international symposium on the digital object; 2009. P. 656–60.
[122] Luo X, Wu B, Liu S. Effects of moist environments on LED module reliability. IEEE Trans Dev Mater Reliab 2010;10:182–6.
[123] Gladkov A, Bar-Cohen A. Parametric dependence of fatigue of electronic adhesives. IEEE Trans Compon Pack Technol 1999;22:200–8.
[124] Kim H-H, Choi S-H, Shin S-H, Lee Y-K, Choi S-M, Yi S. Thermal transient characteristics of die attach in high power LED PKG. Microelectron Reliab 2008;48:445–54.
[125] Hu J, Yang L, Shin MW. Mechanisms and thermal effect of delamination in light-emitting diode packages. Microelectron J 2007;38:157–63.
[126] Mura G, Cassanelli G, Fantini F, Vanzi M. Sulfur-contamination of high power white LED. Microelectron Reliab 2008;48:1208–11.
[127] Wong EH, Chan KC, Rajoo R, Lim TB. The mechanics and impact of hygroscopic swelling of polymeric materials in electronic packaging. ASME J Electron Pack 2002;124:122–6.
[128] Wang L, Feng S, Guo C, Zhang G. Analysis of degradation of GaN-based light-emitting diodes. 16th IEEE IPFA; 2009. p. 472–5.
[129] Rencz M, Szekely V, Morelli A, Villa C. Determining partial resistances with transient measurements, and using the method to detect die attach discontinuities. 18th annual IEEE symposium of semiconductor thermal measurement; 2002. p. 15–20.
[130] Hu J, Yang L, Shin MW. Thermal and mechanical analysis of high-power LEDs with ceramic packages. IEEE Trans Dev Mater Reliab 2008;8:297–303.
[131] Rencz M, Szekely V. Structure function evaluation of stacked dies. 20th annual IEEE semiconductor thermal measurement and management symposium; 2004. p. 50–4.
[132] Hu J, Yang L, Shin MW. Electrical, optical, and thermal degradation of high power GaN/InGaN light-emitting diodes. J Phys D: Appl Phys 2008;41: 1–4.
[133] Molnar G, Nagy G, Szücs Z. A novel procedure and device to allow comprehensive characterization of power LEDs over a wide range of temperature. THERMINIC 2008:89–92.
[134] Tan L, Li J, Wang K, Liu S. Effects of defects on the thermal and optical performance of high-brightness light-emitting diodes. IEEE Trans Electron Pack Manuf 2009;32:233–40.

[135] Yu JH, Farkas G, Vader QV. Transient thermal analysis of power LEDs at package & board level. THERMINIC 2005:244–8.
[136] Arik M, Weaver S. Effect of chip and bonding defects on the junction temperatures of high-brightness light-emitting diodes. Opt Eng 2005;44:11305–1-11305-8.
[137] Driel WDV, Wisse G, Chang AYL, Jassen JHJ, Fan X, Zhang KGO, et al. Influence of material combinations on delamination failures in a cavity-down TBGA package. IEEE Trans Compon Pack Technol 2004;27:651–8.
[138] Driel WDV, van Gils MAJ, Fan X, Zhang GQ, Ernst LJ. Driving mechanisms of delamination related reliability problems in exposed pad packages. IEEE Trans Compon Pack Technol 2008;31:260–8.
[139] Lin Y, Tran N, Zhou Y, He Y, Shi F. Materials challenges and solutions for the packaging of high power LEDs. IMPACT 2006:1–4.
[140] Noor YM, Tam SC, Lim LEN, Jana S. A review of the Nd:YAG laser marking of plastic and ceramic IC packages. J Mater Process Technol 1994;42:95–133.
[141] Vandevelde B, Degryse D, Beyne E, Roose E, Corlatan D, Swaelen G, et al. Modified micro-macro thermo-mechanical modeling of ceramic ball grid array packages. Microelectron Reliab 2003;43:307–18.
[142] Li H-T, Hsu C-W, Chen K-C. The study of thermal properties and thermal resistant behaviors of siloxane-modified LED transparent encapsulant. IMPACT 2007:246–9.
[143] Torikai A, Hasegawa H. Accelerated photodegradation of poly(vinyl chloride). Polym Degrad Stabil 1999;63:441–5.
[144] Narendran N, Gu Y, Freyssinier JP, Yu H, Deng L. Solid-state lighting: failure analysis of white LEDs. J Cryst Growth 2004;268:449–56.
[145] Down JL. The yellowing of epoxy resin adhesives: report on high-intensity light aging. Stud Conserv 1986;31:159–70.
[146] Zhang Q, Mu X, Wang K, Gan Z, Luo X, Liu S. Dynamic mechanical properties of the transient silicone resin for high power LED packaging. ICEPT-HDP; 2008. p. 1–4.
[147] Meneghini M, Trevisanello L-R, Meneghesso G, Zanoni E. A review on the reliability of GaN-based LEDs. IEEE Trans Dev Mater Reliab 2008;8:323–31.
[148] Baillot R, Deshayes Y, Bechou L, Buffeteau T, Pianet I, Armand C, et al. Effects of silicone coating degradation on GaN MQW LEDs performances using physical and chemical analysis. Microelectron Reliab 2010;50:1568–73.
[149] Barton DL, Osinski M. Degradation mechanisms in GaN/AlGaN/InGaN LEDs and LDs. Proceedings of the 10th SIMC-X; 1998. p. 259–62.
[150] Down JL. The yellowing of epoxy resin adhesives: report on natural dark aging. Stud Conserv 1984;29:63–76.
[151] Allen SC, Steckl AJ. A nearly ideal phosphor-converted white light-emitting diode. Appl Phys Lett 2008;92:1433091–93.
[152] Tran NT, Shi FG. Simulation and experimental studies of phosphor concentration and thickness for phosphor-based white light-emitting diodes. IMPACT 2007:255–7.
[153] Arik M, Weaver S, Becker CA, Hsing M, Srivastava A. Effects of localized heat generations due to the color conversion in phosphor conversion in phosphor particles and layers of high brightness light emitting diodes. ASME international electronic packaging technical conference and exhibition; 2003. p. 1–9.
[154] Narendran N, Gu Y, Freyssinier-Nova JP, Zhu Y. Extracting phosphor-scattered photons to improve white LED efficiency. Phys Status Solidi A 2005;202:R60–2.
[155] Kim JK, Luo H, Shubert EF, Cho J, Sone C, Park Y. Strongly enhanced phosphor efficiency in GaInN white light-emitting diodes using remote phosphor configuration and diffuse reflector cup. Jpn J Appl Phys 2005;44:L649–51.
[156] Luo H, Kim JK, Shubert EF, Cho J, Sone C, Park Y. Analysis of high-power packages for phosphor-based white-light-emitting diodes. Appl Phys Lett 2005;86:2435051–53.
[157] Li Y-Q, Fu S-Y, Mai Y-W. Preparation and characterization of transparent ZnO/epoxy nanocomposites with high-UV shielding efficiency. Polymer 2006;47:2127–32.
[158] Schubert EF. Light-emitting diodes. 2nd ed. New York: Cambridge University Press; 2006 [chapter 11].
[159] Hsu Y-C, Lin Y-K, Chen M-H, Tsai C-C, Kuang J-H, Huang S-B, et al. Failure mechanisms associated with lens shape of high-power LED modules in aging test. IEEE Trans Electron Dev 2008;55:570–1.
[160] Arik M, Setlur A, Weaver S, Haitko D, Petroski J. Chip to system levels thermal needs and alternative thermal technologies for high brightness LEDs. J Electron Pack 2007;129:328–38.
[161] Xie R-J, Hirosaki N. Silicon-based oxynitride and nitride phosphors for white LEDs-a review. Sci Technol Adv Mater 2007;8:588–600.
[162] Xie R-J, Hirosaki N, Kimura N, Sakuma K, Mitomo M. 2-phosphor-converted white light-emitting diodes using oxynitride/nitride phosphors. Appl Phys Lett 2007;90:1911011–13.
[163] Jia D, Jia W, Jia Y. Long persistent alkali-earth silicate phosphors doped with Eu2+, ND3+. J Appl Phys 2007;101:0235201–06.
[164] Xie R-J, Hirosaki N, Mitomo M, Takahashi K, Sakuma K. Highly efficient white-light-emitting diodes fabricated with short-wavelength yellow oxynitride phosphors. Appl Phys Lett 2006;88:1011041–43.
[165] Nakamura S. Present performance of InGaN-based blue/green/yellow LEDs. Proc SPIE 1997;3002:26–35.
[166] Tsai C-C, Wang J, Chen M-H, Hsu Y-C, Lin Y-J, Lee C-W, et al. Investigation of Ce:YAG doping effect on thermal aging for high-power phosphor-converted white-light-emitting diodes. IEEE Trans Dev Mater Reliab 2009;9:367–71.
[167] Tang Y-S, Hu S-F, Lin CC, Bagkar NC, Liu R-S. Thermally stable luminescence of KSrPO4:Eu2+ phosphor for white light UV light-emitting diodes. Appl Phys Lett 2007;90:1511081–83.
[168] Mueller-Mach R, Mueller GO, Krames MR. Phosphor materials and combinations for illumination grade white pcLED. Proc SPIE 2003;5187:115–22.
[169] Mueller-Mach R, Mueller GO, Krames MR, Trottier T. High-power phosphor-converted light-emitting diodes based on III-nitrides. IEEE J Sel Top Quantum Electron 2002;8:339–45.
[170] Mueller GO, Mueller-Mach R. White-light-emitting diodes for illumination. Proc SPIE 2000;3938:30–41.
[171] Mueller-Mach R, Mueller G, Krames MR, Hoppe HA, Stadler F, Schnick W, et al. Highly efficient all-nitride phosphors-converted white light emitting diode. Phys Status Solidi A 2005;202:1727–32.
[172] Uheda T, Hirosaki N, Yamamoto Y, Naito A, Nakajima T, Yamamoto H. Luminescence properties of a red phosphor, $CaAlSiN_3:Eu^{2+}$, for white light-emitting diodes. Electrochem Solid-State Lett 2006;9:H22–5.
[173] Li YQ, van Steen JEJ, van Krevel JWH, Botty G, Delsing ACA, Disalvo FJ, et al. Luminescence properties of red-emitting $M_2 Si_5 N_8:Eu^{2+}$ (M=Ca, Sr, Ba) LED conversion phosphors. J Alloys Compd 2006:273–9.
[174] Xie R-J, Hirosaki N, Sakuma K, Kimura N. White light-emitting diodes (LEDs) using (oxy)nitride phosphors. J Phys D: Appl Phys 2008;41: 1440131–35.
[175] Xie R-J, Hirosaki N, Suehiro T, -F Xu F, Mitomo M. A simple, efficient synthetic route to $Sr_2 Si_5 N_8:Eu^{2+}$ based red phosphors for white light-emitting diodes. Chem Mater 2006;18:5578–83.
[176] Zeng Q, Tanno H, Egoshi K, Tanamachi N, Zhang S. $Ba_5 SiO_4 Cl_6:Eu^{2+}$: an intense blue emission phosphor under vacuum ultraviolet and near-ultraviolet excitation. Appl Phys Lett 2006;88:0519061–63.
[177] Misra S, Kolbe J. Reliability of thermal management substrates for LEDs. Electronic design online conference series, session 1; June 22nd, 2010. p. 1–27.
[178] Hong E, Narendran N. A method for projecting useful life of LED lighting systems. Third international conference on solid state lighting, proceedings of SPIE 5187; 2004. p. 93–9.
[179] Qi H, Vichare NM, Azarian MH, Pecht M. Analysis of solder joint failure criteria and measurement techniques in the qualification of electronic products. IEEE Trans Compon Pack Technol 2008;31:469–77.
[180] Guidelines for Accelerated Reliability Testing of Surface Mounting Solder Attachments, IPC-SM-785. The Institute for Interconnecting and Packaging Electronic Circuits, Northbrook, IL; November 1992.
[181] Chang M-H, Das D, Lee SW, Pecht M. Concerns with interconnect reliability assessment of high power light emitting diodes (LEDs). SMTA China south technical conference; 2010. p. 63–9.
[182] Choubey A, Yu H, Osterman M, Pecht M, Yun F, Yonghong L, et al. Intermetallics characterization of lead-free solder joints under isothermal aging. J Electron Mater 2008;37:1130–8.
[183] Li GY, Chen BL. Formation and growth kinetics of interfacial intermetallics in Pb-free solder joint. IEEE Trans Compon Pack Technol 2003;26:651–8.
[184] Osterman M, Pecht M. Strain range fatigue life assessment of lead-free solder interconnects subject to temperature cycle loading. Solder Surf Mount Technol 2007;19:12–7.
[185] Chauhan P, Osterman M, Pecht M. Critical review of the Engelmaier model for solder joint creep fatigue reliability. IEEE Trans Compon Pack Technol 2009;32:693–700.
[186] George E, Das D, Osterman M, Pecht M, Otte C. Physics of failure based virtual testing of communications hardware. A SME IMECE 2009; 2009. p. 121811–18.
[187] Ralston JM, Mann JW. Temperature and current dependence of degradation in red-emitting GaP LED's. J Appl Phys 1979;50:3630–7.
[188] Bergh AA. Bulk degradation of GaP red LEDs. IEEE Trans Electron Dev 1971;18:166–70.
[189] Meneghini M, Podda S, Morelli A, Pintus R, Trevisanello L, Meneghesso G, et al. High brightness GaN LEDs degradation during DC and pulsed stress. Microelectron Reliab 2006;46:1720–4.
[190] Tan CM, Eric Chen BK, Foo YY, Chan RY, Xu G, Liu YJ. Humidity effect on the degradation of packaged ultra-bright white LEDs. 10th electronics packaging technology conference; 2008. p. 1–6.
[191] Hu J, Yang L, Shin M. Mechanical and thermal effect of delamination in light-emitting diode packages. Microelectron J 2007;38:157–63.
[192] Tan CM, Chen BKE, Xu G, Liu Y. Analysis of humidity effects on the degradation of high-power white LEDs. Microelectron Reliab 2009;49:1226–30.
[193] Narendran N, Gu Y. Life of LED-based white light sources. IEEE/OSA J Disp Technol 2005;1:167–71.
[194] Trevisanello L, Zuani FD, Meneghini M, Trivellin N, Zanoni E, Meneghesso G. Thermally activated degradation and package instabilities of low flux LEDs. 2009 IEEE international reliability physics symposium; 2009. p. 98–103.
[195] Bar-Cohen A, Kraus AD. Advances in thermal modeling of electronic components and systems, vol. 4. New Jersey: ASME Press; 1998.
[196] Gao S, Hong J, Shin S, Lee Y, Choi S, Yi S. Design optimization on the heat transfer and mechanical reliability of high brightness light emitting diodes (HBLED) package. 58th ECTC 2008; 2008. p. 798–803.
[197] Jayasinghe L, Gu Y, Narendran N. Characterization of thermal resistance coefficient of high-power LEDs. 6th international conference on solid state lighting, proceedings of SPIE; 2006. p. 1–10.

[198] Gu Y, Narendran N. A non-contact method for determining junction temperature of phosphor-converted white LEDs. 3rd international conference on solid state lighting, proceedings of SPIE 5187; 2004. p. 107–14.
[199] Sanawiratne J, Zhao W, Detchprohm T, Chatterjee A, Li Y, Zhu M, et al. Junction temperature analysis in green light emitting diode dies on sapphire and GaN substrates. Phys Status Solidi C 2008;5:2247–9.
[200] Chhajed S, Xi Y, Li Y-L, Gessmann Th, Schubert EF. Influence of junction temperature on chromaticity and color-rendering properties of trichromatic white-light sources based on light-emitting diodes. J Appl Phys 2005;97:0545061–68.
[201] Chen ZZ, Liu P, Qi SL, Lin L, Pan HP, Qin ZX, et al. Junction temperature and reliability of high-power flip-chip light emitting diodes. Mater Sci Semicond Process 2007;10:206–10.
[202] Liu J, Tam WS, Wong H, Filip V. Temperature-dependent light-emitting characteristics of InGaN/GaN diodes. Microelectron Reliab 2009;49:38–41.
[203] Peng L-H, Chuang C-W, Lou L-H. Piezoelectric effects in the optical properties of strained InGaN quantum wells. Appl Phys Lett 1999;74:795–7.
[204] Casey Jr HC, Muth J, Krishnankutty S, Zavada JM. Dominance of tunneling current and band filling in InGaN/AlGaN double heterostructure blue light-emitting diodes. Appl Phys Lett 1996;68:2867–9.
[205] Lasance CJM, Poppe A. Challenges in LED thermal characterisation. EuroSimE; 2009. p. 1–11.
[206] Poppe A, Lasance CJM. On the standardization of thermal characterization of LEDs. In: 25th IEEE SEMI-THERM symposium; 2009. p. 1–8.
[207] Poppe A, Lasance CJM. On the standardisation of thermal characterisation of LEDs part II: problem definition and potential solutions. THERMINIC; 2008. p. 213–9.
[208] Poppe A, Lasance CJM. Hot topic for LEDs: standardization issues of thermal characterization. Light and lighting conference with special emphasis on LEDs and solid state lighting, Budapest, Hungary, CIE; 2009. p. 1–4.
[209] Poppe A, Molnár G, Temesvölgyi T. Temperature dependent thermal resistance in power LED assemblies and a way to cope with it. 26th IEEE SEMI-THERM symposium; 2010. p. 1–6.
[210] Lasance CJM. Thermally driven reliability issues in microelectronic systems: status-quo and challenges. Microelectron Reliab 2003;43:1969–74.
[211] Joshi Y, Azar K, Blackburn D, Lasance CJM, Mahajan R, Rantala J. How well can we assess thermally driven reliability issues in electronic systems today? Summary of panel held at the therminic 2002. Microelectron J 2003:1195–201.
[212] Lasance CJM. Ten years of boundary-condition-independent compact thermal modeling of electronic parts: a review. Heat Transfer Eng 2008;29:149–68.
[213] Lasance CJM. The conceivable accuracy of experimental and numerical thermal analyses of electronic systems. 17th IEEE SEMI-THERM symposium; 2001. p. 180–98.
[214] Lasance CJM. The European project profit: prediction of temperature gradients influencing the quality of electronic products. 17th IEEE SEMI-THERM symposium; 2001. p. 120–5.